Journal of Food and Drug Analysis

Volume 31 | Issue 1 Article 8

Guilu Erxian Jiao enhances protein synthesis, glucose homeostasis, mitochondrial biogenesis and slow-twitch fibers in the skeletal muscle

Recommended Citation
Fang, Wei-Yu; Chang, Wan-Hsuan; Tsai, Yi-Hong; Hsu, Hung-Te; Chang, Fang-Rong; Lin, Chih-Lung; and Lo, Yi-Ching (2023) "Guilu Erxian Jiao enhances protein synthesis, glucose homeostasis, mitochondrial biogenesis and slow-twitch fibers in the skeletal muscle," *Journal of Food and Drug Analysis*: Vol. 31 : Iss. 1 , Article 8.
Available at: https://doi.org/10.38212/2224-6614.3435

This Original Article is brought to you for free and open access by Journal of Food and Drug Analysis. It has been accepted for inclusion in Journal of Food and Drug Analysis by an authorized editor of Journal of Food and Drug Analysis.

ORIGINAL ARTICLE

Guilu Erxian Jiao enhances protein synthesis, glucose homeostasis, mitochondrial biogenesis and slow-twitch fibers in the skeletal muscle

Wei-Yu Fang [a], Wan-Hsuan Chang [a,b], Yi-Hong Tsai [c], Hung-Te Hsu [d], Fang-Rong Chang [c], Chih-Lung Lin [e,f], Yi-Ching Lo [a,b,c,f,g,*]

[a] Department of Pharmacology, School of Medicine, College of Medicine, Kaohsiung Medical University, Kaohsiung 80708, Taiwan
[b] Graduate Institute of Medicine, College of Medicine, Kaohsiung Medical University, Kaohsiung 80708, Taiwan
[c] Graduate Institute of Natural Products, College of Pharmacy, Kaohsiung Medical University, Kaohsiung 80708, Taiwan
[d] Faculty of Anesthesiology, School of Medicine, College of Medicine, Kaohsiung Medical University, Kaohsiung 80708, Taiwan
[e] Department of Neurosurgery, Kaohsiung Medical University Hospital, Kaohsiung 80708, Taiwan
[f] Department of Medical Research, Kaohsiung Medical University Hospital, Kaohsiung 80708, Taiwan
[g] School of Pharmacy, College of Pharmacy, Kaohsiung Medical University, Kaohsiung 80708, Taiwan

Abstract

Guilu Erxian Jiao (GEJ) is a commonly used nutritional supplement due to its rich content of amino acids. It is also a traditional herbal medicine for improving degenerative joint. This study aimed to investigate the effect and mechanism of GEJ water extract (GEJ-WE) on skeletal muscle in C2C12 myotubes and C57BL/6J mice. Analysis of GEJ-WE were performed by high-performance liquid chromatography fingerprinting with chemical standards. Protein expression, mRNA level, glycogen content, mitochondria activity and ATP level were evaluated by western blots, real-time PCR, PAS staining, MTT and ATP bioluminescence assay, respectively. Skeletal muscle strength was evaluated by grip strength. Skeletal muscle volume, mass and fiber types were evaluated by micro computed tomography, histological analysis and immunofluorescence staining, respectively. Motor function was evaluated by rotarod performance and locomotor activity. In C2C12 myotubes, GEJ-WE significantly enhanced myogenic differentiation and myotube growth, protein synthesis signaling IGF-1/IGF-1R/IRS-1/Akt, Glut4 translocation, glycogen content, mitochondrial biogenesis signaling PGC-1α/NRF1/TFAM, mitochondrial activity and ATP production. However, IGF-1R antagonist AG1024 and PI3K inhibitor wortmannin reduced GEJ-WE-induced protein expression of MyHC, p-Akt, p-mTOR and p-GSK-3β, Glut4 translocation and glycogen content. In C57BL/6J mice, GEJ-WE not only upregulated protein synthesis and mitochondrial biogenesis signaling, but it also increased muscle volume, relative muscle weight, cross-sectional area of myofibers, glycogen content and transition of fast-to-slow type fibers of skeletal muscles. Moreover, GEJ-WE enhanced grip strength and motor activity of mice. In conclusion, the upregulation of protein synthesis, myogenic differentiation, glucose homeostasis, mitochondrial biogenesis and slow-twitch fibers contributes to the mechanisms of GEJ-WE on the enhancement of skeletal muscle mass and motor function.

Keywords: Guilu Erxian Jiao, Glucose homeostasis, Mitochondrial biogenesis, Muscle mass, Protein synthesis

1. Introduction

Skeletal muscle is the most abundant tissue in the human body. Skeletal muscle mass is determined largely by the balance of muscle protein synthesis and degradation, which is regulated by nutritional and physiological factors [1]. Evidence reveals that maintaining skeletal muscle mass is not only integral for breathing and locomotion, but is also clinically important to regulate metabolic systems [2,3]. In addition, significant muscle wasting, malnutrition and clinical cachexia are observed in patients with coronavirus disease 2019 (COVID-19) [4]. Skeletal muscle consists of heterogenous fibers which can categorized into two groups based on the presence of

Received 9 May 2022; accepted 24 August 2022.
Available online 15 March 2023

* Corresponding author. Department of Pharmacology, School of Medicine, College of Medicine, Kaohsiung Medical University, 100 Shih-Chuan 1st Road, Kaohsiung 80708, Taiwan. Fax: +886 7 3234686.
E-mail address: yichlo@kmu.edu.tw (Y.-C. Lo).

https://doi.org/10.38212/2224-6614.3435

the myosin heavy chain (MyHC) subtypes: the slow-twitch (type I) fibers and the fast-twitch (type II) fibers [5]. Slow-twitch fibers are mitochondrial-rich and fatigue resistant, whereas fast-twitch fibers contain fewer mitochondrial and are low endurance [6]. Importantly, the increased proportion of slow-twitch fibers is negatively correlated with disease-related muscle atrophy [7]. Therefore, increasing the proportion of slow-twitch fibers enhances muscle endurance and maintains muscle functions.

Insulin-like growth factor 1 (IGF-1)/type 1 IGF receptor (IGF-1R) signaling plays a crucial role in muscle protein synthesis, differentiation, and regeneration [1]. IGF-1 activates its receptor IGF-1R, leading to the recruitment and activation of adaptor protein insulin receptor substrate-1 (IRS-1). The activated IRS-1 then induces downstream phosphatidylinositol 3-kinase (PI3K)/Akt signaling and further promotes protein synthesis via phosphorylating the mammalian target of rapamycin complex 1 (mTORC1) and glycogen synthase kinase 3β (GSK-3β) [8]. In addition, IGF-1/Akt is an important regulator to promote glucose uptake into muscle cells. Activation of IGF-1/Akt enhances the membrane translocation of glucose transporter type 4 (Glut4), the major glucose transporter expressed in skeletal muscle, and then increased glucose uptake [9]. The increased intracellular level of glucose can either produce adenosine triphosphate (ATP) by mitochondria or store as glycogen for energy reservoir.

Mitochondrial dysfunction is one of the major causes involved in skeletal muscle atrophy [10]. Mitochondria are critical eukaryotic organelles that possess many important functions including ATP generation, intracellular signaling regulation and oxidative-antioxidant system balance. Peroxisome proliferator-activated receptor gamma coactivator-1α (PGC-1α) is the key regulator of mitochondrial biogenesis in skeletal muscle [11]. Co-activation of PGC-1α with nuclear respiratory factors 1 (NRF1) promotes the expression of mitochondrial transcription factor A (TFAM), leading to transcription and replication of mitochondrial DNA [11]. The increase of mitochondrial biogenesis results in sufficient ATP supply, with the consequence of favoring metabolism and maintaining muscle mass and functions [10].

Guilu Erxian Jiao (GEJ), a widely used amino acid-rich dietary supplement and traditional herbal medicine, possesses multiple pharmacological activities including anti-inflammation [12] and anti-oxidation [13]. Amino acid is not only an important energy source but also contributes to the protein synthesis in the skeletal muscle [14]. Amino acid supplement also serves as a potential therapeutic strategy for attenuating skeletal muscle atrophy through activation of the protein synthesis pathway [15]. GEJ consists of ventral shells of *Chrysemys scripta elegans* Testudinidae (TCP), ossified antlers from *Cervus elaphus* L., Cervidae (CCP), dried roots and rhizomes of *Panax ginseng* C. A. Meyer, Araliaceae (GR) and dried mature fruits of *Lycium barbarum* L., Solanaceae (LF) in a ratio of 5:10:1:2. GEJ is also a well popular amino acid-rich dietary supplement [16] without serious adverse effects after long-term taking [17]. Previous study reported that Guilu Erxian Glue (GEG), a GEJ similar formula, can be a protective and alternative therapy for alleviating doxorubicin-induced weight loss, motor disability, blood circulation defects, and bone loss [13]. Due to the ratio of ingredients TCP, CCP, GR and LF in GEJ (5:10:1:2) and GEG (4:2:1:2) were inconsistent, the proportion of active components of GEJ and GEG is also somewhat different. It has been reported that patients with knee osteoarthritis who received GEJ treatment for 12 weeks significantly increased muscle strength [18]. Some ingredients and main components of GEJ have been reported their beneficial effects on skeletal muscles. Ginseng extracts [19] and CCP [20] possess beneficial effects on muscle endurance and muscle grip strength in normal mice. Ginseng extracts regulates neurotransmitters and improves neuromuscular dysfunctions [21]. Ginsenoside Rb1 and Rb2 promote differentiation and myotube growth via accelerating MyoD and MyoE protein heterodimerization and Akt/mTOR signaling respectively in C2C12 myoblasts [22]. In addition, ginsenoside Rb1 can increase glycogen synthesis [23]. In TNF-α-induced myotube atrophy, ginsenoside Rg3 increases differentiation and activates Akt/mTOR signaling [24]. Betaine, the main bioactive compound of LF, is an amino-acid derivative, which can increase glycogen synthesis [25] and myoblast differentiation and PGC-1α-mediated mitochondrial biogenesis [26]. Increasing evidence indicates that betaine is associated with therapeutic potential in insulin-sensitive tissues, such as skeletal muscle, adipose tissue, and liver [27]. However, the mechanism of action of GEJ on skeletal muscle remains unclear. In this study, we quantitatively analyzed GEJ water extract (GEJ-WE) and further revealed the novel mechanisms of GEJ-WE on skeletal muscle using *in vitro* and *in vivo* models.

2. Materials and methods

2.1. Materials

AG1024, dimethyl sulfoxide (DMSO), trypan blue solution, wortmannin, 3-(4, 5-dimethylthiazol-2-yl)-

2,5-diphenyl-tetrazolium bromide (MTT) were purchased from Sigma–Aldrich Chemical Co. (St. Louis, MO, USA). Dulbecco's modified Eagle's medium (DMEM), fetal bovine serum (FBS), Fast SYBR green master mix, horse serum, high-capacity cDNA reverse transcription kit, penicillin and streptomycin, TRIzol reagent, T-PER tissue protein extraction reagent and Alexa Fluor 488 goat anti-mouse IgG secondary antibody were purchased from Thermo Fisher Scientific (Waltham, MA, USA). All materials used for sodium dodecyl sulfate-polyacrylamide gel electrophoresis (SDS-PAGE) were purchased from Bio-Rad (Hercules, CA, USA). Plasma membrane extraction kit was purchased from BioVision (Mountain View, CA, USA). Enhanced chemiluminescence (ECL) detection kit and polyvinylidene difluoride (PVDF) membrane were purchased from Millipore (Billerica, MA, USA). Luminescent ATP detection assay kit was purchased from Abcam (Cambridge, MA, USA). Lactate dehydrogenase (LDH) cytotoxicity assay kit was obtained from G-Biosciences (St. Louis, MO, USA). Antibodies used in this study were indicated as follows: β-actin (Sigma–Aldrich); MyHC (R&D Systems); GAPDH, p-GSK-3β (Ser9), MYH2, MYH7, NRF1, mtTFA, anti-rabbit IgG-HRP and anti-mouse IgG-HRP were obtained from Santa Cruz Biotechnology; IGF-1R, p-IGF-1R (Tyr1135), IRS-1, GSK-3β, p-Akt (Ser473), Akt, p-mTOR (Ser2448), mTOR were obtained from Cell Signaling Technology; PGC-1α (Novus). Chemical reference standards for high-performance liquid chromatography (HPLC) fingerprinting were indicated as follows: L-hydroxyproline (99%, Nacalai Tesque Inc., Japan), Glycine (99.9% U. S. Pharmacopeia, USA), DL-alanine (99%, Acros Organics, Belgium) and L-proline (99.9%, Nacalai Tesque Inc., Japan). Ginsenoside Rg1 (93.4%), ginsenoside Re (92.3%), ginsenoside Rb1 (91.2%), ginsenoside Rc (98.59%), ginsenoside Rd (94.2%) and betaine (100%) were purchased from the National Institutes for Food and Drug Control, China. All the materials of GEJ were purchased from the Chuang Song Zong Pharmaceutical Co., Ltd. Ligang Plant (Pingtung, Taiwan), which meet the international standard of EU GMP guide.

2.2. Guilu Erxian Jiao water extract (GEJ-WE) preparation and analysis

The GEJ-WE was prepared as follows: TCP 500 g and CCP 1000 g were kept in a slightly boiling state in purified water (the quality of water complies with EP monograph 2249 water for preparation of extracts) for 7 days, then steamed GR 100 g and LF 200 g were added and the decoction is continued for a period of time. After that, the extract was filtered out and concentrated under reduced pressure to obtain the semisolid, GEJ-WE (858.6 g, yield: 43.4%). Amino acids in GEJ-WE were qualitatively and quantitatively analyzed with a HPLC system, Waters® 2695 Separations Module consisted with Waters® 2996 Photodiode Array (PDA) Detector. Detail analytic parameters were optimized as follows, Column: Cosmosil® 5C18 -AR-II, 120 Å, 5 μm, 4.6 × 250 mm; Mobile phases: (A) 93% of 0.1 mol/L sodium acetate trihydrate (Millipore Sigma, USA) (pH = 6.5 adjusted with diluted acetic acid) and 7% of HPLC grade acetonitrile (LiChrosolv®, Merck KGaA, Germany); (B) 80% of HPLC grade acetonitrile and 20% of water (ultrapure, made with Millipore Synergy 185 Lab water purification system, Merck KGaA, Germany); gradient program: 0–30 min, from 100% of (A) to 25% of (A); column oven temperature: 43 °C; flow rate: 1.0 mL/min; detecting wavelength: UV 254 nm. Ginsenosides in GEJ-WE were investigated with an HPLC system of Waters® 2695 Separations Module and Waters® 2998 Photodiode Array (PDA) Detector. Detail analytic parameters were as follows, Column: Cosmosil® 5C18-AR-II, 120 Å, 5 μm, 4.6 × 250 mm (Nacalai Tesque Inc., Japan); Mobile phases: (A) 0.15% H_3PO_4 in water; (B) HPLC grade acetonitrile; gradient program: 0–105 min, from 81% of (A) to 60% of (A); column oven temperature: 15 °C; flow rate: 1.0 mL/min; detecting wavelength: UV 203 nm. The exact content of betaine in GEJ-WE was quantified with the same HPLC system as amino acid analysis in this work. Detail analytic parameters were as follows, Column: ZORBAX® Original NH2, 70 Å, 5 μm, 4.6 × 250 mm (Agilent Technologies, Inc., USA); Mobile phases: isocratic H_2O: HPLC grade acetonitrile = 15:85 for 60 min; column oven temperature: 30 °C; flow rate: 1.0 mL/min; detecting wavelength: UV 195 nm.

2.3. Evaluation of lipopolysaccharide levels

The GEJ-WE was tested for bacterial lipopolysaccharide (LPS) by the ToxinSensor™ Chromogenic LAL Endotoxin Assay Kit. (GenScript, Piscataway, NJ, USA). Briefly, GEJ-WE was diluted with LAL Reagent Water to 1 μg/mL and reacted with reconstituted limulus amebocyte lysate at 37 °C for 30 min following with the addition of substrate. The absorbance at 545 nm was measured by an ELISA reader. The endotoxin level was calculated based on comparison to the *Escherichia coli* endotoxin standard reference.

2.4. Cell culture and drug treatment

C2C12 myoblasts (#KCB 2012115 YJ) were purchased from the Bioresource Collection and Research Center (Hsinchu, Taiwan) and cultured in DMEM containing 10% FBS, 100 U/ml penicillin and 100 μg/mL streptomycin at 37 °C in a humidified incubator with 5% CO_2. When cells reached 80% of the confluence, the medium was replaced by differentiation medium (DMEM containing 2% horse serum) and changed every other day for 6 days to form myotubes. The differentiated C2C12 myotubes were treated with or without GEJ-WE (0.01, 0.05, 0.1, 0.5 and 1 μg/mL) for 8 h or 24 h. For antagonist treatments, cells were pre-treated with IGF-1R antagonist AG1024 (10 nM, dissolved in 0.1% DMSO) or PI3K/Akt inhibitor wortmannin (100 nM, dissolved in 0.1% DMSO) for 1 h before GEJ-WE treatment.

2.5. Animal preparation and drug treatment

Seven to eight-week old male C57BL/6J mice (23–25 g) were purchased from the National Laboratory Animal Center (Taipei, Taiwan). All animal work was performed in an Association for Assessment and Accreditation of Laboratory Animal Care International (AAALAC)-accredited facility of Kaohsiung Medical University. Mice were acclimatized for 1 week after arrival and housed 3 per cage under a 12 h dark–light cycle at 22 ± 1 °C with *ad libitum* food and water. All experiments were approved by the Animal Care and Use Committee of the Kaohsiung Medical University (IACUC approval No. 107152). Mice were randomly separated into four groups (6 mice per group): control group (vehicle (saline)-treated group); GEJ-WE (100 mg/kg/day) group; GEJ-WE (200 mg/kg/day) group; GEJ-WE (300 mg/kg/day) group. The doses used in the current study were similar with previous mice study [12] and were lower than other human studies [18,28] when convert to human equivalent dosage according to the body surface area-based dose-conversion guidance [29]. The fasting blood glucose level, blood pressure and heart rate were measured every 2 weeks. The body weight and food intake were measured every two days and an equal amount of food was given at the same time after measurement. Previous studies have shown that after 4 weeks of feeding some herbal medicine can increase muscle strength and weight in normal mice [19,30]. Accordingly, in this study, after 4 weeks of feeding GEJ-WE, muscle strength and motor activity were measured. Then, mice were euthanized with CO_2 and the gastrocnemius, tibialis anterior and rectus femoris muscles were collected for protein extraction and histological analysis.

2.6. LDH cytotoxicity assay

The cytotoxicity was evaluated by measuring the released LDH into the culture medium using LDH cytotoxicity assay kit. Briefly, C2C12 myoblasts (6×10^4 cells/well) were seeded in a 96-well plate and differentiated for 6 days. Myotubes were incubated with GEJ-WE for 24 h. Media were then transferred to another 96-well plate following the addition of Substrate Mixture. The plate was incubated at 37 °C in the dark for 30 min and then terminated by Stop Solution. The absorbance at 490 nm was measured by an ELISA reader.

2.7. Mitochondrial activity measurement

Mitochondrial activity was measured by MTT assay. Briefly, C2C12 myoblasts (6×10^4 cells/well) were seeded in a 96-well plate and differentiated for 6 days. Myotubes were incubated with GEJ-WE for 24 h, then culture medium were replaced with fresh medium containing MTT (0.5 mg/mL) and incubated in the dark for 3 h at 37 °C. A parallel plate was also prepared for cell number determination by the trypan blue exclusion assay and confirmed that the number of cells were comparable after GEJ-WE treatment. The formazan crystals were dissolved with DMSO and the absorbance was measured at 540 nm and 630 nm by an ELISA Reader.

2.8. Quantitative RT-PCR (qRT-PCR)

C2C12 myotubes were treated with GEJ-WE for 8 h. Total RNA was extracted using TRIzol reagent and cDNA was synthesized from 1 μg RNA using High-Capacity cDNA Reverse Transcription Kit. PCR reaction was performed using StepOnePlus™ Real-Time PCR System (Thermo Fisher Scientific, Waltham, MA, USA) with Fast SYBR Green Master Mix. The mRNA level of Igf-1 was normalized to the level of the housekeeping gene glyceraldehyde-3-phosphate dehydrogenase (Gapdh). Specific primers and sequences were as follows: Gapdh forward primer 5′-TGTCAAGCTCATTTCCTGGT-3′, reverse primer 5′-TAGGGCC-TCTCTTGCTC-AGT-3’; Igf-1 forward primer 5′-GGACCGAGGGGCTTTTACTT-3′, reverse primer 5′-TCCGGAAGCAACACTCA-TCC-3’.

2.9. Western blot analysis

Samples were lysed by T-PER Tissue Protein Extraction Reagent. The supernatant was collected and quantified the protein concentration. Membrane and cytosol protein extracts were isolated

using commercial membrane protein extraction kit (BioVision). Equal amounts of protein were loaded in SDS-PAGE and transferred onto PVDF membranes. Membranes were blocked with 5% non-fat milk in TBST (50 mM Tris–HCl, pH 7.6, 150 mM NaCl, 0.1% Tween 20) for 1 h at room temperature and then incubating with primary antibodies (diluted 1:1000 in blocking buffer) at 4 °C overnight followed by incubated with HRP-conjugated secondary antibody (diluted 1:10,000 in 5% non-fat milk) at room temperature for 1 h. The immunoreactivity was detected using Amersham ECL detection kit. The intensities of protein bands were quantitated using Image J software.

2.10. Total cellular ATP levels measurement

Total cellular ATP levels were measured using the Luminescent ATP Detection Assay Kit (Abcam) according to the manufacturer's instructions. Briefly, C2C12 myotubes were incubated with GEJ-WE for 24 h. The detergent was added to lyse the cells and stabilize the ATP. Equal amount of substrate buffer was added and the luminescence absorbance was measured using the BioTek Synergy H1 microplate reader (BioTek, Winooski, VT, USA). The ATP concentration was calculated based on comparison to the standard reference.

2.11. Skeletal muscle histology

The gastrocnemius, tibialis anterior and rectus femoris muscles were collected and fixed overnight in 10% formalin, then dehydrated and embedded in paraffin. The embedded tissue blocks were sectioned into 5-μm thickness and stained with hematoxylin and eosin (H&E) staining for measuring myofiber cross-sectional area (CSA) or periodic acid-schiff (PAS) staining for measuring glycogen content by standard methods. The paraffin-embedded tissue sections from the same batch used for measurement of myofiber CSA were further used to examine the effects of GEJ-WE on lipid content by Oil Red O staining, according to the method described in supplementary information. Images were captured under a optical microscopy (ECLIPSE 80i, Nikon, Japan) at 200× magnification and analyzed by ImageJ software. The mean myofiber CSA were measured in five randomly selected images with 50–80 fibers per image per mouse.

2.12. Immunofluorescence staining

For staining of C2C12 myotubes, myotubes were fixed with 4% paraformaldehyde in PBS (pH 7.4) for 10 min at room temperature, and then permeabilized by incubating with 0.2% Triton X-100 in PBS for 15 min. Myotubes were blocked in 3% BSA in PBS for 1 h at room temperature and then incubated with mouse anti-MyHC antibody (1:1000) at 4 °C for overnight. The next day, myotubes were incubated with Alexa Fluor 488-conjugated secondary antibody (1:1000) for 1 h at room temperature. Myonuclei were stained by DAPI and images were observed under fluorescence microscopy (Nikon, Japan) at 100× magnification. ImageJ software was used to measure myotube number, myotube length and myotube diameter from five randomly selected fields of each sample type.

For staining of type I and II muscle fibers, tissue sections were deparaffinized and rehydrated, then permeabilized with 0.2% Triton X-100 in PBS for 30 min at room temperature. Sections were then blocked with 2% bovine serum albumin in PBS for 1 h, followed by incubating primary antibody for slow-twitch (type I) fiber (MYH7, diluted 1:1000) or fast-twitch (type II) fiber (MYH2, diluted 1:1000) at 4 °C overnight. After washing by PBS, sections were incubated with Alexa Fluor 488-conjugated secondary antibodies (diluted 1:1000) at room temperature for 1 h. Nuclei were stained with DAPI and observed under fluorescence microscopy (Nikon, Japan) at 200× magnification. The percentage of each fiber type were manually counted and calculated as total number of each fiber type/total number of fibers counted from five randomly selected fields for each sample.

2.13. Micro computed tomography (Micro-CT) analysis

Micro-CT analysis was performed for assessing the muscle volume according to our previous report [31]. The right tibia of each mouse was scanned before treatment (baseline) and after GEJ-WE treatment for 4 weeks, using micro-CT (SkyScan 1076, Kontich, Belgium) without contrast agents. Mice were anesthetized with a continuous flow of 3% isoflurane/oxygen mixture and placed prone during scanning. The subsequent reconstruction work was performed using NRecon, Data Viewer, and CTvol SkyScan software.

2.14. Whole limb grip strength measurement

A grip strength meter (Bio-GS3, BioSeb, Vitrolles, France) was used to assess the whole limb grip strength of the mice according to our previous report [32]. Mice were lifted by the tail and induced to grasp a rigid grids attached to a digital force gauge. The tail of each mouse was gently pulled

backwards and the tension reading of the digital force gauge was defined as the grip strength before the mouse released the net. Five consecutive tests were performed on each mouse and the mean maximum whole limb muscle strength value (grams) (g) was calculated as absolute grip strength. The relative grip strength was calculated as absolute grip strength (g)/body weight (g).

2.15. Rotarod performance test

Mice were trained to walk on the accelerating rotarod apparatus (Orchid Scientifics) before the GEJ-WE treatment. The speed of the rod was linearly increased from 3 rpm to 30 rpm during 60 s. The time of the mice fell off the device were recorded automatically.

2.16. Locomotor activity

Each mouse was placed in the center of a chamber (50 cm × 50 cm × 25 cm) and allowed to freely explore the chamber for 30 s, followed by a 5-min test, the total travel distance (mm) and the mean velocity (mm/s) of each mouse were recorded and analyzed by VideoTrack analysis system (ViewPoint Behavior Technology).

2.17. Statistical analysis

Data from the analysis of chemical components of GEJ-WE were from three different batches and expressed as mean ± SD. Data from cellular and animal studies were generated from 6 independent *in vitro* experiments or 6 mice per group (n = 6, where n represented the number of independent values as reported in each figure legend) and expressed as mean ± SEM. All statistical analyses were performed using SPSS17 statistical software (SPSS Inc., Chicago, IL, USA). Differences were analysed one-way ANOVA followed by a Tukey post hoc or Kruskal–Wallis test followed by Dunn's test for multiple comparisons. Statistical significance was considered as $p < 0.05$. *P* value for statistical significance was not varied later in Results. For reducing unwanted sources of variation, we used 'percentage matched control values' to normalize the data of MTT assay, western blotting and qRT-PCR experiments.

3. Results

3.1. Analysis of chemical components of GEJ-WE

As shown in Fig. 1, the 3D-HPLC profiles of GEJ-WE were showed as chromatograms of amino acids

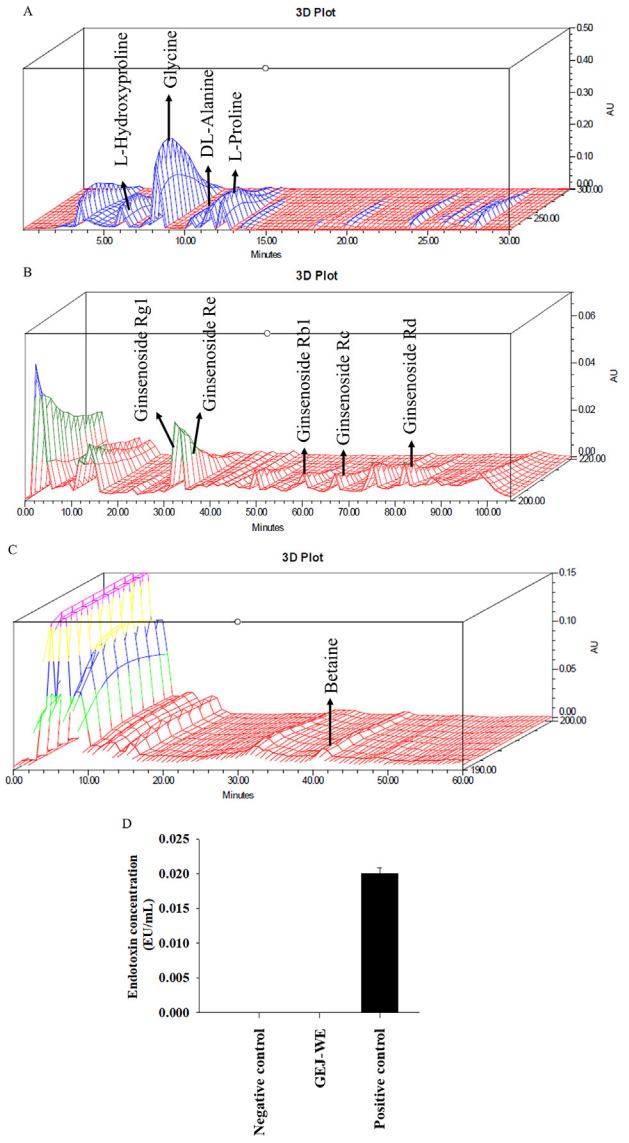

Fig. 1. The three-dimensional HPLC chromatograms and endotoxin (lipopolysaccharide) concentration of GEJ-WE. Standardization of GEJ-WE was done using HPLC fingerprinting with chemical standards. HPLC chromatogram of amino acids in GEJ-WE (A). HPLC chromatogram of ginsenosides in GEJ-WE (B). HPLC chromatogram of betaine in GEJ-WE (C). The GEJ-WE was tested for measuring the lipopolysarcchride concentration using the Endotoxin Assay Kit (D). LAL Reagent Water is shown as a negative control, and 0.02 EU/mL endotoxin is shown as a positive control. Data represent the mean ± SEM from six independent experiment (n = 6).

(Fig. 1A), ginsenosides (Fig. 1B) and betaine (Fig. 1C), and the content of chemical components in GEJ-WE were shown in Table 1: L-hydroxyproline (50.90 ± 0.02 mg/g), glycine (111.26 ± 0.88 mg/g), DL-alanine (46.99 ± 0.05 mg/g), L-proline (63.04 ± 0.21 mg/g), ginsenoside Rg1 (0.74 ± 0.01 mg/g), ginsenoside Re (0.36 ± 0.01 mg/g), ginsenoside Rb1 (0.36 ± 0.01 mg/g), ginsenoside Rc (0.42 ± 0.01 mg/g), ginsenoside Rd (0.27 ± 0.01 mg/g)

Table 1. Linearity of calibration curves and determination of active compounds in GEJ-WE.

Components	Contents (mg/g)	Regression equation	Regression coefficient	Linear Range (mg/g)	Precision (RSD)	Accuracy (Recovery %)
L-Hydroxyproline	50.90 ± 0.02	y = 6259.5x+6756.6	r^2 = 0.9999	11.30~113.04	0.50%	99.77%
Glycine	111.26 ± 0.88	y = 10142x-1486.9	r^2 = 0.9999	18.07~180.65	0.40%	101.05%
DL-Alanine	46.99 ± 0.05	y = 8522.4x-11985	r^2 = 0.9999	7.96~79.58	0.80%	98.84%
L-Proline	63.04 ± 0.21	y = 7188.8x+2224.5	r^2 = 0.9998	13.93~139.27	0.40%	101.86%
Ginsenoside Rg1	0.74 ± 0.01	y = 2620x+1101.2	r^2 = 0.9999	0.38~3.82	1.40%	101.99%
Ginsenoside Re	0.36 ± 0.01	y = 5194.5x-3065.3	r^2 = 0.9999	0.15~1.53	0.70%	102.03%
Ginsenoside Rb1	0.36 ± 0.01	y = 4269.8x-12892	r^2 = 0.9968	0.19~1.87	0.40%	95.10%
Ginsenoside Rc	0.42 ± 0.01	y = 4605.9x-18878	r^2 = 0.9994	0.20~2.05	0.90%	101.83%
Ginsenoside Rd	0.27 ± 0.01	y = 3694.4x-2691.6	r^2 = 0.9998	0.14~1.41	0.80%	100.80%
Betaine	2.51 ± 0.00	y = 3825.3x-21748	r^2 = 0.9997	1.71~8.55	0.50%	101.51%

and betaine (2.51 ± 0.00 mg/g). The data of method validation including the assessment of linearity, range, precision and accuracy for quantitative analysis on GEJ-WE were listed in Table 1. We further confirmed the absence of LPS in GEJ-WE as shown in Fig. 1D.

3.2. Effects of GEJ-WE on myotube growth

First, we confirmed that GEJ-WE (0.01–1 μg/mL) did not cause cytotoxicity in C2C12 myotubes by LDH assay (Fig. 2A). Therefore, we performed the study with this dosage range. We found GEJ-WE significantly increased the MyHC protein expression (Fig. 2B). In addition, ginsenoside Rg1, one of the active compounds in GEJ-WE, also upregulated MyHC protein expression in C2C12 myotubes (Fig. 2B). To further investigate the effects of GEJ-WE on C2C12 myotube growth, we measured the number, length and diameter of myotubes by immunofluorescence staining with MyHC antibody (Fig. 2C). GEJ-WE significantly increased the

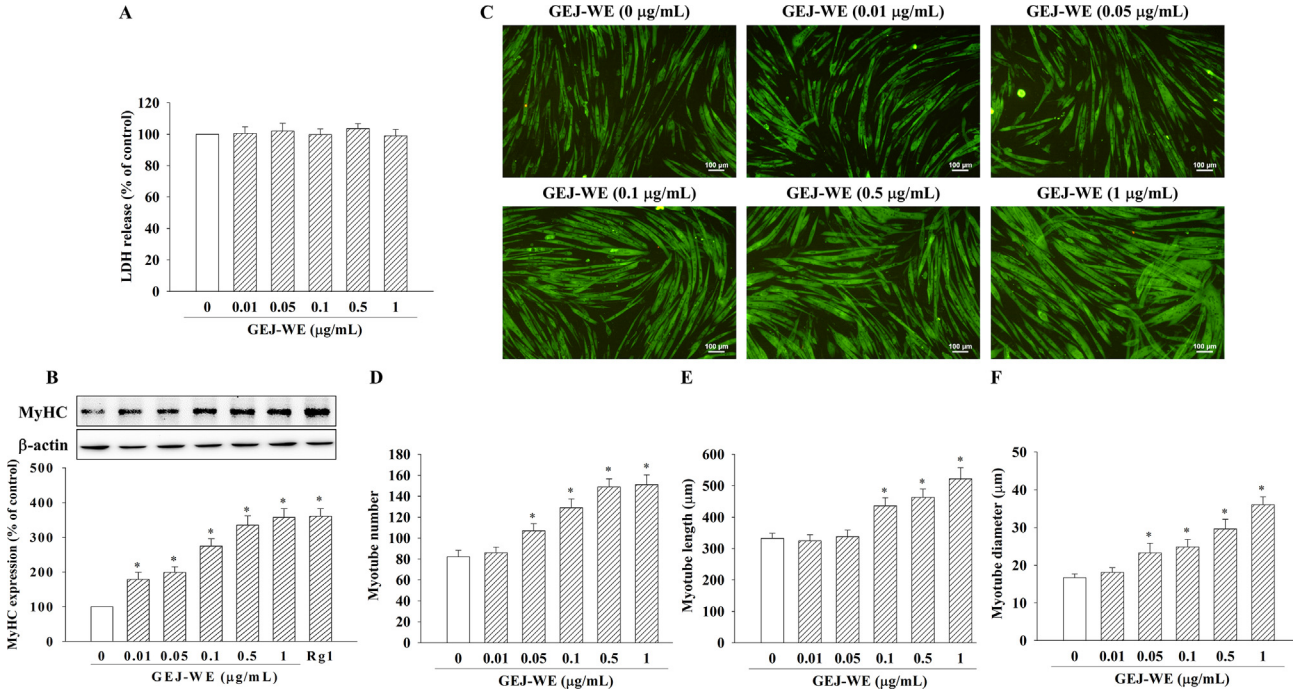

*Fig. 2. **Effects of GEJ-WE on cytotoxicity (A), MyHC expression (B) and growth (C–F) of C2C12 myotubes.** Cells were treated with GEJ-WE (0.01, 0.05, 0.1, 0.5 and 1 μg/mL) for 24 h. Cytotocixity was determined by the LDH assay. Total protein was extracted for measuring expressions of MyHC by western blotting. MyHC staining was performed to visualize mature myotube structure and evaluated the myotube growth including myotube number, myotube length and myotube diameter. Scale bar = 100 μm. Densitometry analyses are presented as the relative ratio of protein/β-actin and are represented as percentages of matched control group. Ginsenoside Rg1 (10 nM) was dissolved in 0.1% DMSO. Data represent the mean ± SEM from six independent experiments (n = 6). *p < 0.05 vs. control group (without GEJ-WE treatment) according to Kruskal–Wallis test followed by Dunn's test.*

number (Fig. 2D), length (Fig. 2E) and diameter (Fig. 2F) of myotubes.

3.3. Effects of GEJ-WE on protein synthesis signaling and glucose homeostasis of C2C12 myotubes

Next, we examined the effects of GEJ-WE protein synthesis IGF-1/IGF-1R signaling. As shown in Fig. 3A and G, GEJ-WE upregulated total and phosphorylated IGF-1R protein. It also upregulated IRS-1 (Fig. 3B and G) accompanied with upregulating the phosphorylation of Akt and mTOR (Fig. 3C, D and 3G). In addition, GEJ-WE upregulated p-GSK-3β (Ser9) (Fig. 3E and 3G). Moreover, GEJ-WE increased the IGF-1 mRNA level (Fig. 3F). We also examined the effects of GEJ-WE on the glucose homeostasis in C2C12 myotubes. As shown in Fig. 4A, GEJ-WE decreased cytosolic Glut4 expression while increased Glut4 translocation to plasma membrane. Besides, we found GEJ-WE increased glycogen content in C2C12 myotubes identified by PAS staining (Fig. 4B and C). However, GEJ-WE-induced upregulation of MyHC, phosphorylated Akt, mTOR and GSK-3β were attenuated by IGF-1R antagonist AG1024 (10 nM) or PI3K inhibitor wortmannin (100 nM) (Fig. 5A-D and H). The enhancing effects of GEJ-WE on Glut4 translocation (Fig. 5E and H) and glycogen content (Fig. 5F and G) were also reduced by AG1024 or wortmannin.

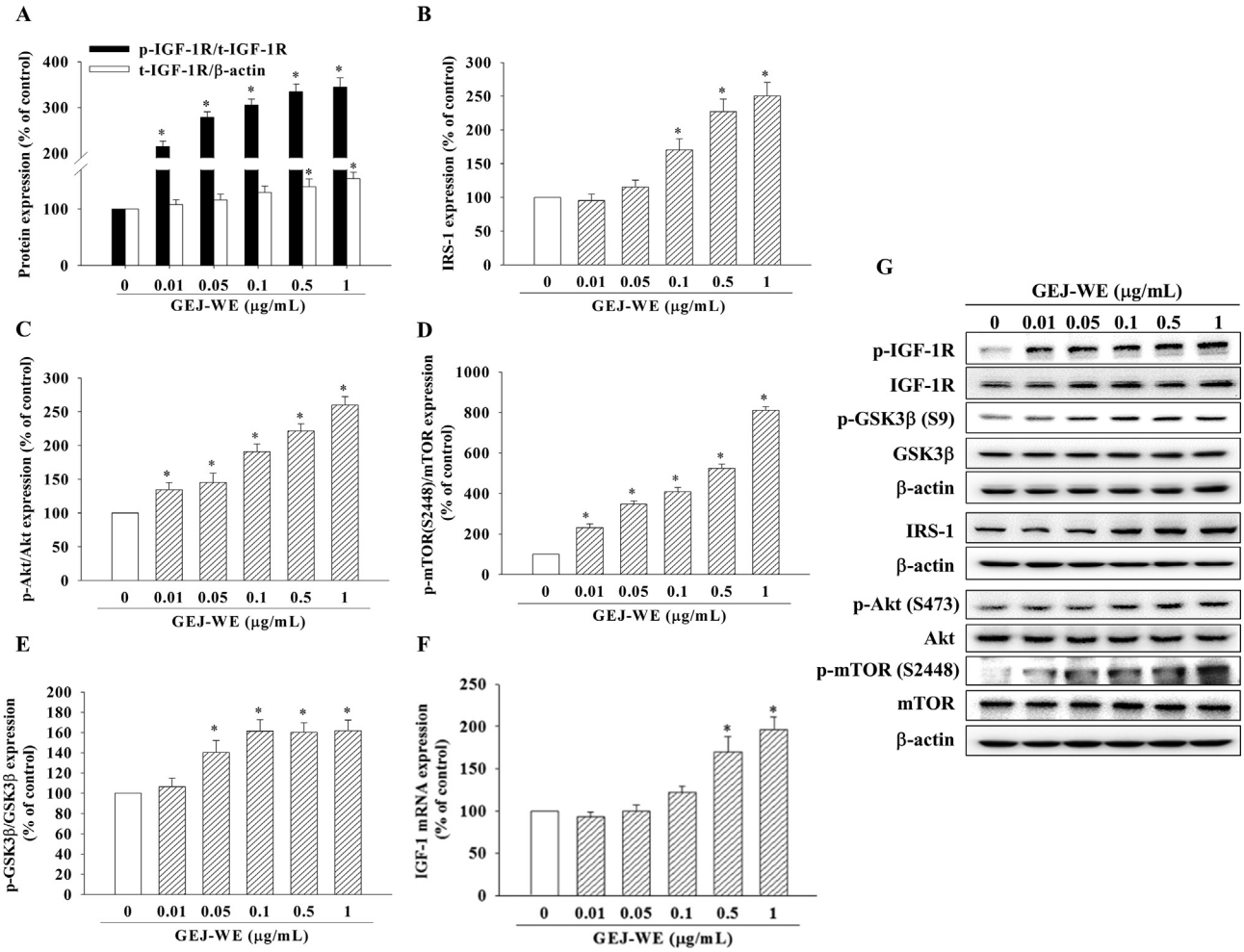

*Fig. 3. Effects of GEJ-WE on protein expression of protein expression of p-IGF-1R/IGF-1R (A), IRS-1 (B), p-Akt (S473)/Akt (C), p-mTOR (S2448)/mTOR (D), p-GSK-3β (S9)/GSK-3β (E) and mRNA expression of IGF-1 (F) in C2C12 myotubes. Cells were treated with GEJ-WE (0.01, 0.05, 0.1, 0.5 and 1 μg/mL) for 24 h. Total proteins were then extracted, and the expression of proteins were measured by western blotting (G). For IGF-1 mRNA expression, cells were treated with GEJ-WE (0.01, 0.05, 0.1, 0.5 and 1 μg/mL) for 8 h and then extracted RNA for measuring IGF-1 mRNA by qPCR. Densitometry analyses are presented as the relative ratio of protein/β-actin or p-protein/protein, and are represented as percentages of matched control group. Data represent the mean ± SEM from six independent experiments (n = 6). *p < 0.05 vs. control group (without GEJ-WE treatment) according to Kruskal–Wallis test followed by Dunn's test.*

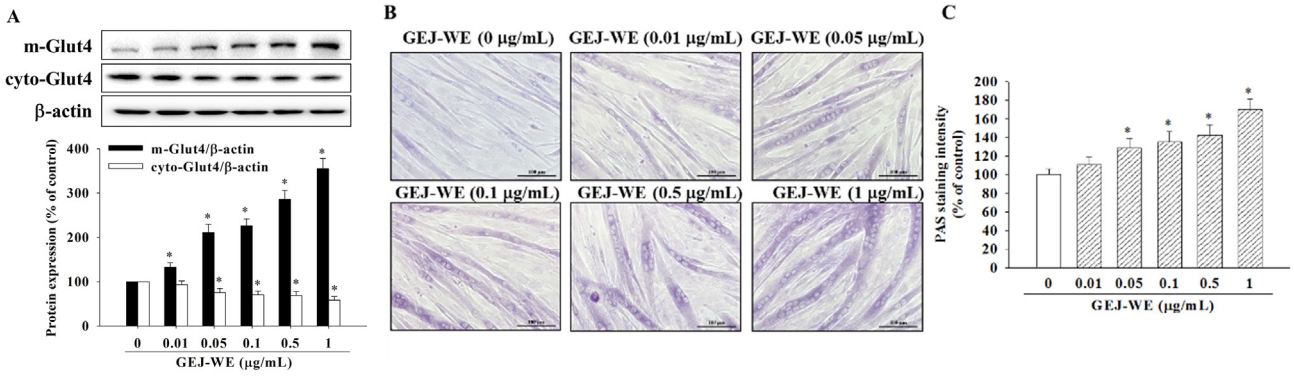

*Fig. 4. **Effects of GEJ-WE on Glut4 translocation (A) and glycogen content (B and C) in C2C12 myotubes.** Cells were treated with GEJ-WE (0.01, 0.05, 0.1, 0.5 and 1 μg/mL) for 24 h. Protein expressions of membrane (m-Glut4) and cytosolic glucose transporter 4 (cyto-Glut4) were measured by western blotting. Glycogen contents were measured by PAS staining and quantified the intensity by image]. Densitometry analyses are presented as the relative ratio of protein/β-actin and are represented as percentages of matched control group. Data represent the mean ± SEM from six independent experiments (n = 6). *p < 0.05 vs. control group (without GEJ-WE treatment) according to Kruskal–Wallis test followed by Dunn's test.*

3.4. Effects of GEJ-WE on mitochondrial biogenesis signaling and ATP production of C2C12 myotubes

As shown in Fig. 6A, GEJ-WE upregulated the protein expressions of PGC-1α as well as the downstream target NRF1 and TFAM (Fig. 6B and C). In addition, ginsenoside Rg1-induced upregulation of PGC-1α was also observed (Fig. 6A). We further examined the effects of GEJ-WE on mitochodrial activity and ATP production of C2C12 myotubes. As shown in Fig. 6D and E, GEJ-WE significantly increased mitochondrial activity and ATP levels of C2C12 mytoubes.

3.5. Effects of GEJ-WE on physiological parameters, skeletal muscle strength and motor performance of C57BL/6J mice

The mice were randomly separated into four groups: control (vehicle) group; GEJ-WE (100 mg/kg/day) group; GEJ-WE (200 mg/kg/day) group; GEJ-WE (300 mg/kg/day) group. Mice were orally treated with vehicle (saline) or GEJ-WE for 4 weeks. We found that GEJ-WE (100, 200, 300 mg/kg) did not change the growth curve of mice when compared with control group during the treatment (Fig. S1). The effects of GEJ-WE on body weight, food intake, blood pressure, heart rate and blood glucose level of mice were shown in Table 2. Compared with the control group, GEJ-WE treatment had no significant effects on body weight, food intake, blood pressure and heart rate. However, GEJ-WE reduced fasting blood glucose levels of mice. Moreover, GEJ-WE (100, 200 and 300 mg/kg/day) increased absolute muscle grip strength and relative muscle grip strength of mice at 4-weeks post GEJ-WE treatment (Fig. 7A and B). GEJ-WE (200 and 300 mg/kg/day) also increased total travelled distance of mice (Fig. 7C and D). Furthermore, in rotarod test, GEJ-WE (300 mg/kg/day) increased latency to fall of mice (Fig. 7E).

3.6. Effects of GEJ-WE on volume, weight, fiber cross-sectional area and lipid content of skeletal muscle in C57BL/6J mice

The right tibia of each mouse was scanned before treatment (baseline) and after GEJ-WE treatment for 4 weeks by micro-CT, results showed that GEJ-WE (100, 200 and 300 mg/kg/day) significantly increased muscle volumes of mice compared with control group (Fig. 8A and B). GEJ-WE (200 and 300 mg/kg/day) increased the relative muscle weight of gastrocnemius (Fig. 8C), tibialis anterior (Fig. 8D) and rectus femoris muscles (Fig. 8E) of mice compared with control group. In addition, GEJ-WE (200 and 300 mg/kg/day) increased the myofiber CSA in the gastrocnemius, tibialis anterior and rectus femoris muscles compared with control group (Fig. 9) while significantly reduced the lipid content as measured by Oil Red O staining using the same batch paraffin-embedded tissue sections for myofiber CSA measurement (Fig. S2).

3.7. Effects of GEJ-WE on glycogen content, fiber types transition, protein synthesis signalings and mitochondrial biogenesis signaling in mice skeletal muscle

We further examined the effects of GEJ-WE on glycogen content and fiber type composition in mice skeletal muscle. As shown in Fig. 10, GEJ-WE increased the glycogen content in the gastrocnemius, tibialis anterior and rectus femoris muscles

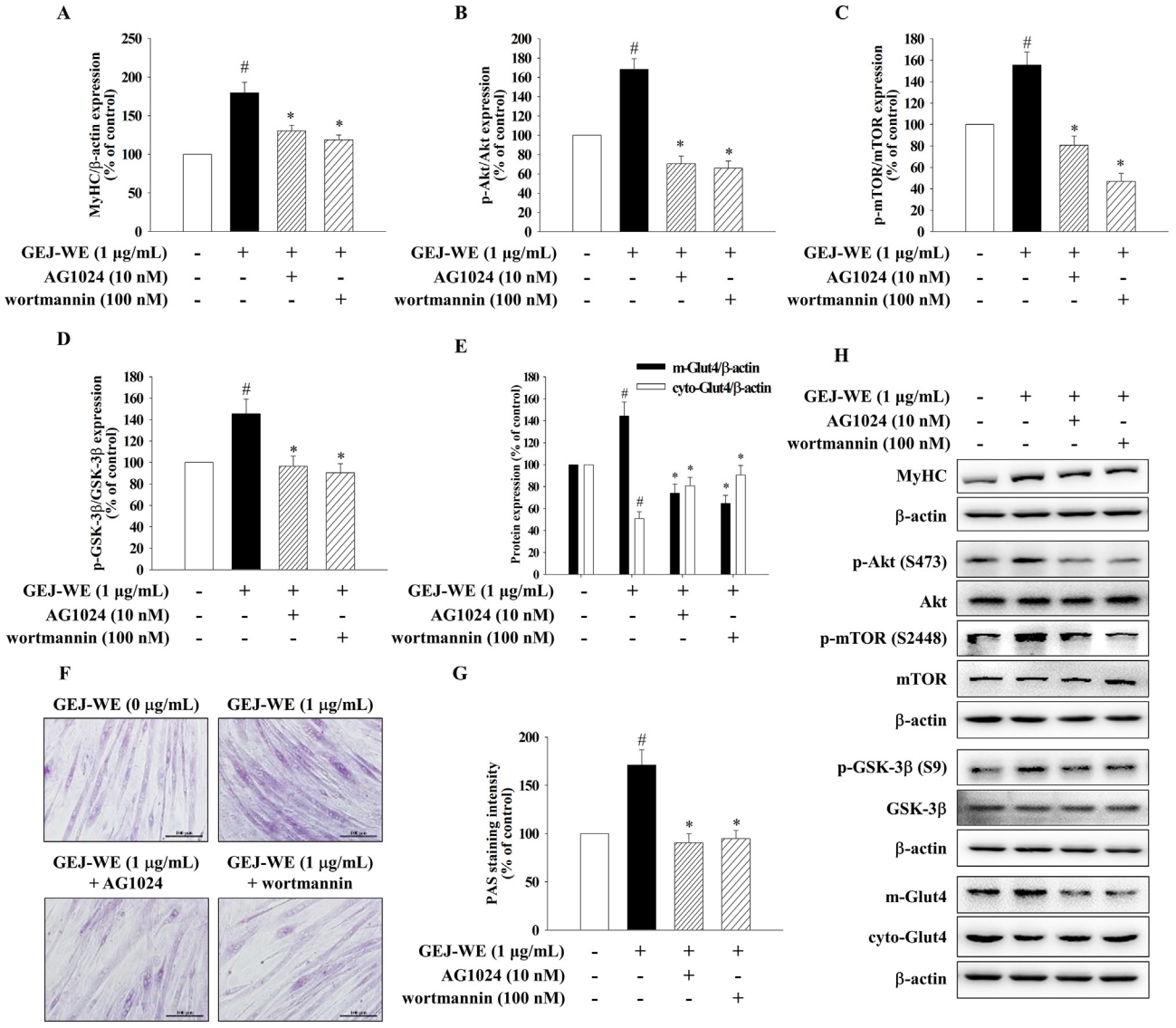

Fig. 5. Effects of AG1024 and wortmannin on GEJ-WE-induced protein expression of MyHC (A), p-Akt (S473)/Akt (B), p-mTOR (S2448)/mTOR (C), p-GSK-3β (S9)/GSK-3β (D) and Glut4 translocation (E) and glycogen contents (F and G) in C2C12 myotubes. Cells were pre-incubated with AG1024 (10 nM) or wortmannin (100 nM) for 1 h following with the addition of GEJ-WE (1 μg/mL) for 24 h. Total proteins were then extracted, and the expression of proteins were measured by western blotting **(H)**. Glycogen contents were measured by PAS staining and quantified the intensity by imageJ. Densitometry analyses are presented as the relative ratio of protein/β-actin or p-protein/protein, and are represented as percentages of matched control group. Data represent the mean ± SEM from six independent experiments ($n = 6$). $^{\#}p < 0.05$ vs. control group without any treatment; $^{*}p < 0.05$ vs. GEJ-WE-treated group according to Kruskal–Wallis test followed by Dunn's test.

compared with the control group. As shown in Fig. 11, GEJ-WE (200 and 300 mg/kg) increased the proportion of slow-twitch (type I) fibers of gastrocnemius muscle from 7.7% (control group: without GEJ-WE treatment) to 19.7% (GEJ-WE 200 mg/kg) and 31.5% (GEJ-WE 300 mg/kg) in a dose-dependent manner, and similar results were also observed in tibialis anterior muscle and rectus femoris muscle. As shown in Fig. 12, GEJ-WE (200 and 300 mg/kg) reduced the proportion of fast-twitch (type II) fibers of gastrocnemius muscle from 55.7% (control group: without GEJ-WE treatment) to 31.6% (GEJ-WE 200 mg/kg) and 15.0% (GEJ-WE 300 mg/kg) in a dose-dependent manner, and similar results were also observed in tibialis anterior muscle and rectus femoris muscle. Moreover, GEJ-WE upregulated protein synthesis signaling IGF-1R/IRS-1/p-Akt/p-mTOR, p-GSK-3β and mitochondrial biogenesis signaling PGC-1α/NRF1/TFAM in skeletal muscle tissue (Fig. 13).

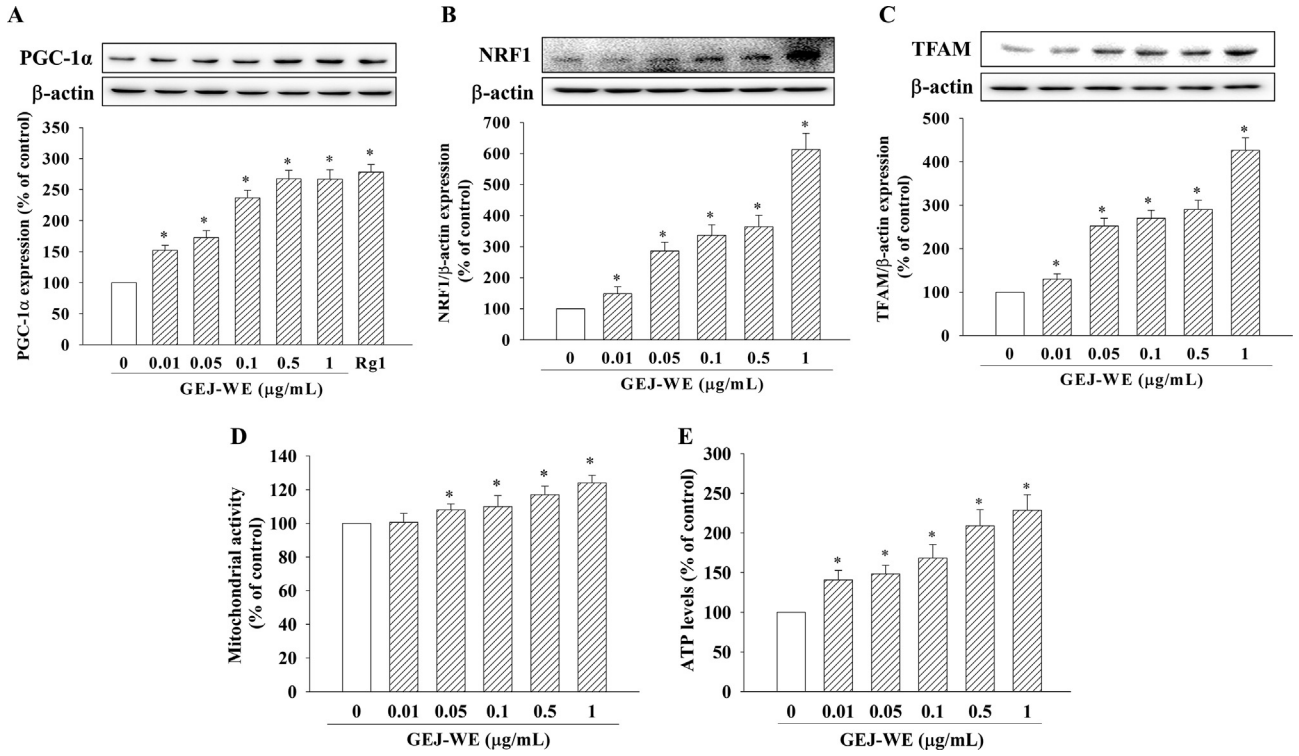

Fig. 6. Effects of GEJ-WE on protein expression of PGC-1α (A), NRF1 (B) and TFAM (C), mitochondrial activity (D) and ATP production (E) in C2C12 myotubes. Cells were treated with GEJ-WE (0.01, 0.05, 0.1, 0.5 and 1 μg/mL) for 24 h. Total proteins were then extracted, and the expression of proteins were measured by western blotting. The mitochindria activity and total cellular ATP levels were measured by MTT assay and ATP bioluminescent assay kit, respectively. Densitometry analyses are presented as the relative ratio of protein/β-actin and are represented as percentages of matched control group. Ginsenoside Rg1 (10 nM) was dissolved in 0.1% DMSO. Data represent the mean ± SEM from six independent experiments ($n = 6$). *$p < 0.05$ vs. control group (without GEJ-WE treatment) according to Kruskal–Wallis test followed by Dunn's test.

Table 2. Effects of GEJ-WE on physiological parameters of C57BL/6 mice.

	Control	GEJ-WE (100 mg/kg)	GEJ-WE (200 mg/kg)	GEJ-WE (300 mg/kg)
Body weight (g)				
Initial	24.80 ± 0.43	24.91 ± 0.37	24.90 ± 0.42	25.30 ± 0.25
2 weeks post treatment	25.61 ± 0.43	25.21 ± 0.36	25.63 ± 0.74	25.86 ± 0.49
4 weeks post treatment	25.70 ± 0.30	25.03 ± 0.23	25.83 ± 0.65	25.95 ± 0.46
Food intake (g/day)	2.26 ± 0.09	2.20 ± 0.01	2.23 ± 0.05	2.21 ± 0.15
SBP (mmHg)				
Initial	131.77 ± 5.45	129.70 ± 3.87	132.39 ± 3.17	131.08 ± 4.81
2 weeks post treatment	132.17 ± 3.16	129.48 ± 3.59	128.35 ± 4.51	130.33 ± 4.62
4 weeks post treatment	129.57 ± 4.60	131.87 ± 3.65	133.46 ± 4.16	130.50 ± 4.40
DBP (mmHg)				
Initial	93.92 ± 6.80	96.16 ± 3.68	95.10 ± 4.85	94.72 ± 5.55
2 weeks post treatment	96.55 ± 5.32	95.46 ± 4.37	96.88 ± 5.64	94.58 ± 5.61
4 weeks post treatment	94.73 ± 4.84	96.92 ± 6.76	95.02 ± 5.25	97.73 ± 4.12
Heart rate (beats/min)				
Initial	377.78 ± 31.73	387.99 ± 30.58	385.92 ± 29.31	380.17 ± 30.67
2 weeks post treatment	388.48 ± 45.41	396.32 ± 51.17	400.29 ± 45.33	388.90 ± 44.41
4 Weeks Post Treatment	387.23 ± 49.43	406.08 ± 52.86	397.77 ± 45.24	390.02 ± 55.15
Fasting blood glucose (mg/dL)				
Initial	170.69 ± 7.69	169.90 ± 6.87	171.11 ± 7.74	168.00 ± 7.85
2 weeks post treatment	174.89 ± 6.25	165.91 ± 7.29	161.64 ± 4.98	161.22 ± 4.63
4 weeks post treatment	178.14 ± 5.08	163.00 ± 7.25	152.29 ± 6.21*	151.14 ± 3.52*

DBP: diastolic blood pressure. SBP: systolic blood pressure, Data represented as mean ± SEM from six independent mice (n = 6 per group). Statistical comparisons were made by one-way ANOVA followed by a Tukey post hoc test. *$p < 0.05$ vs. control group (vehicle (saline)-treated group).

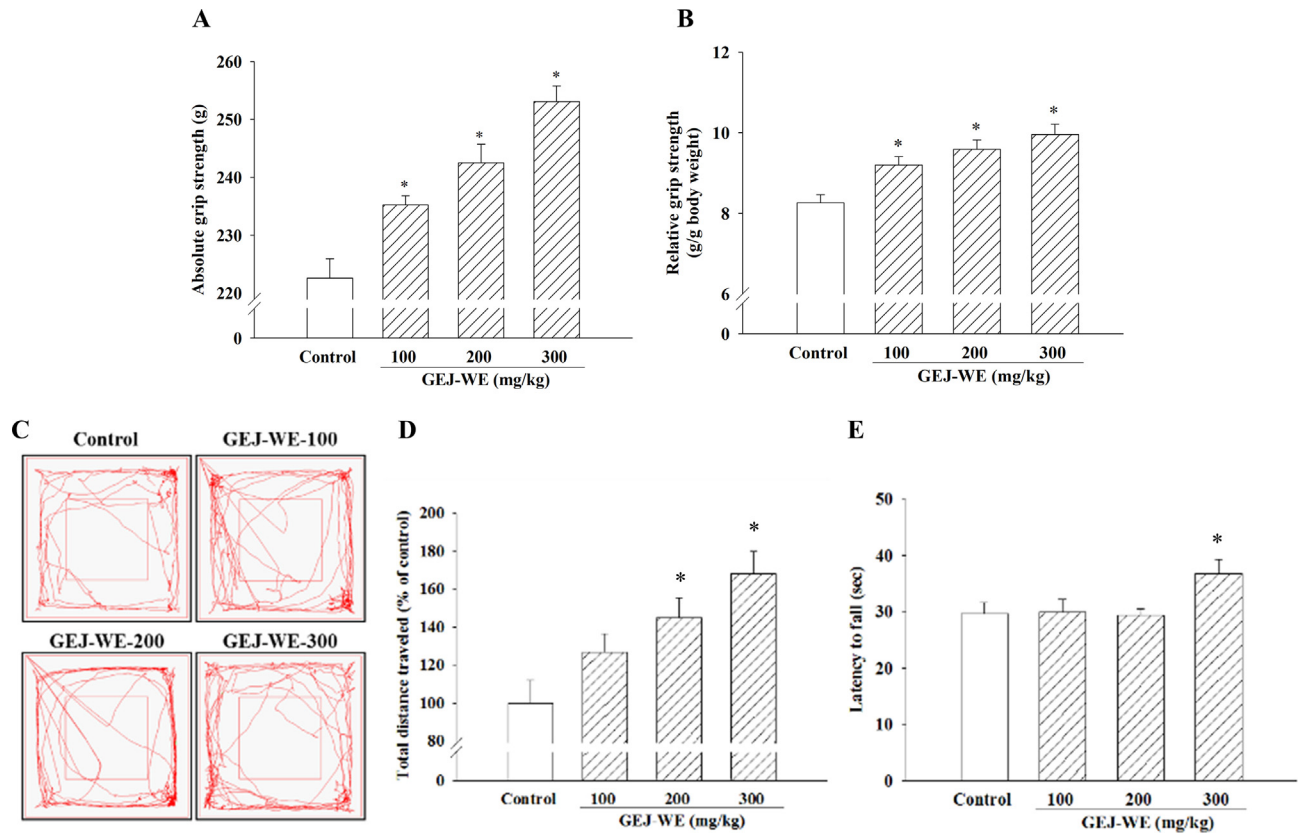

*Fig. 7. Effects of GEJ-WE on absolute grip strength (A), relative grip strength (B), locomotor activity (C and D) and rotarod performance (E) of C57BL/6J mice. Mice were orally treated with vehicle only (saline) or with GEJ-WE (100, 200 and 300 mg/kg/day) for 4 weeks. All tests were evaluated at 4-weeks post GEJ-WE treatment. The maximum whole limb muscle force of mice was measured by grip strength meter and shown as absolute grip strength and relative grip strength (normalized with body weight). For locomotor activity test, trace-paths and total distance of mice were recorded in 5 min. Latency to fall was measured by rotarod performance test. Data represent the mean ± SEM from six independent mice (n = 6 per group). *p < 0.05 vs. control group (vehicle-treated) according to one-way ANOVA followed by a Tukey post hoc test.*

4. Discussion

Skeletal muscle plays a vital role in supporting overall health and wellness. How to maintain skeletal muscle mass and strong has become an important issue. This study first reveals the novel mechanism of GEJ on skeletal muscle mass and function in normal mice. Our results showed that GEJ-WE possesses the novel effects on enhancing myotube growth, skeletal muscle mass, muscle strength and motor activity through regulating myogenic differentiation, protein synthesis, glycogen synthesis, mitochondrial biogenesis and fast-to-slow-twitch fiber type transition.

It is well known that IGF-1/IGF-1R/Akt signaling plays an important role in regulating skeletal muscle homeostasis including myogenic differentiation, protein synthesis, and glucose homeostasis [1,8]. Upregulation of IGF-1/IGF-1R/Akt-mediated skeletal muscle protein synthesis is positively correlated with myotube hypertrophy leading to increased skeletal muscle CSA and mass [1,8]. Skeletal muscle has been identified as a secretory organ [33]. The myokines (e.g., IGF-1) secreted by skeletal muscle play important roles in the communication with other organs and regulation with muscle itself. IGF-1 is abundant in homogenized skeletal muscle tissue and secreted from cultured C2C12 myotubes [34]. Skeletal muscle IGF-1 has a greater effect on skeletal muscle maintenance than liver IGF-1 [35]. In this study, GEJ-WE activated p-IGF-1R/Akt signaling at concentrations ranging from 0.01 to 1.0 μg/mL, whereas increased IGF-1 mRNA expression was observed at concentrations from 0.5 to 1.0 μg/mL. Previous study reported that muscle IGF-1/IGF-1R/Akt signaling can form a positive feedback loop resulting in the synergistically increased expression of IGF-1 itself [36]. Therefore, GEJ-WE-mediated IGF-1/IGF-1R/Akt signaling activation might contribute to the mechanistic evidence involved in

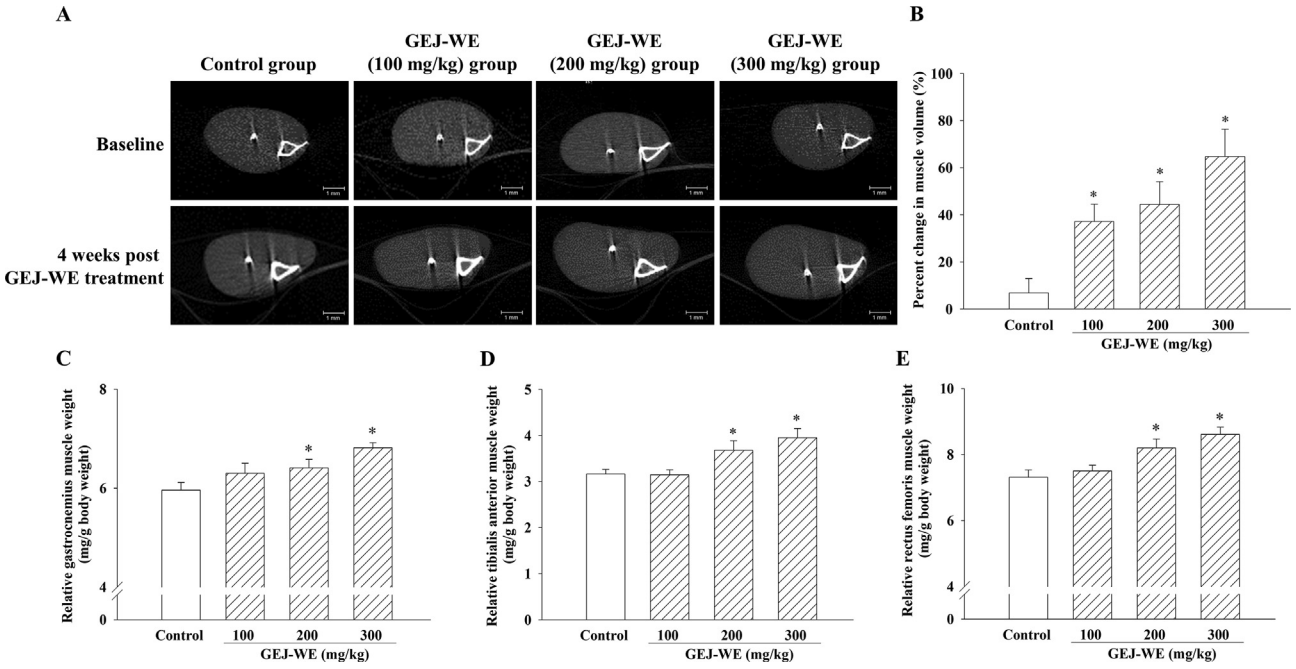

*Fig. 8. Effects of GEJ-WE on muscle volume (A and B) and relative muscle weight (C to E) of C57BL/6J mice. Mice were orally treated with vehicle only (saline) or with GEJ-WE (100, 200 and 300 mg/kg/day) for 4 weeks. Muscle volume was assessed by micro-CT before (baseline) at 4-weeks post GEJ-WE treatment. Scale bars = 1 mm. Muscle volume (mm^3) was calculated as total volume − (tibia volume + fibula volume). The percentage changes in muscle volumes were calculated as (volume (baseline) − volume (post GEJ-WE treatment))/volume (baseline). Relative muscle weight of gastrocnemius muscle (C), tibialis anterior muscle (D) and rectus femoris muscle (E) in each groups was calculated as skeletal muscle weight (mg)/body weight (g). Data represent the mean ± SEM from six independent mice (n = 6 per group). *p < 0.05 vs. control group (vehicle-treated) according to one-way ANOVA followed by a Tukey post hoc test.*

GEJ-WE-induced IGF-1 expression. In addition, GEJ-WE is an amino acid-enriched mixture, and amino acids could increase IGF-1 mRNA and protein expression in human myotubes and skeletal muscle tissues [37]. Moreover, betaine, one of the main active components of GEJ-WE, also activates IGF-1/IGF-1R signaling [38] in C2C12 myotubes. Our results showed that GEJ-WE increased protein expression of IGF-1R, IRS-1, p-Akt, p-mTOR and p-GSK3β in both GEJ-WE-treated C2C12 myotubes (Fig. 3) and GEJ-WE-treated mice skeletal muscle tissues (Fig. 13). Previous studies have found that some active components of GEJ-WE including ginsenoside Rb1 [22], ginsenoside Rg1 [39] and betaine [26] increased C2C12 myogenic differentiation and myotube hypertrophy through Akt activation [22,39], suggesting the potential of these active components on promoting myotube growth. GEJ-WE increased C2C12 myotubes numbers, lengths and diameters as well as terminal myotube maturation marker MyHC expression (Fig. 2). Our results indicated that GEJ-WE significantly increased skeletal muscle volume (Fig. 8B) and relative skeletal muscle weight (Fig. 8C to E). GEJ-WE also increased skeletal muscle mass by measuring cross-sectional area of myofibers (Fig. 9). Moreover, comparing the changes in body weight between the GEJ-WE group and the control group, GEJ-WE had no significant effect on the growth curve of mice (Fig. S1). As shown in Table 2, after feeding mice with GEJ-WE (100, 200, 300 mg/kg) for 4 weeks, no significant difference in body weight gain between GEJ-WE groups and control group. We further confirmed GEJ-WE decreased lipid content in skeletal muscle tissues (Fig. S2). Moreover, our data (Fig. 5) also showed that GEJ-WE-induced upregulation of MyHC, p-mTOR and p-GSK-3β were inhibited by IGF-1R antagonist (AG1024) and Akt antagonist (wortmannin). Therefore, the promoting effects of GEJ-WE on activating IGF-1/IGF-1R/Akt signaling and myogenic differentiation might contribute to the mechanistic evidence involved in GEJ-WE-induced enhancing effects on skeletal muscle mass.

Skeletal muscles are comprised of two major fiber types, slow-twitch (type I) and fast-twitch (type II) fibers. Slow-twitch (type I) fibers have higher mitochondrial content and muscle endurance property than those of fast-twitch (type II) fibers

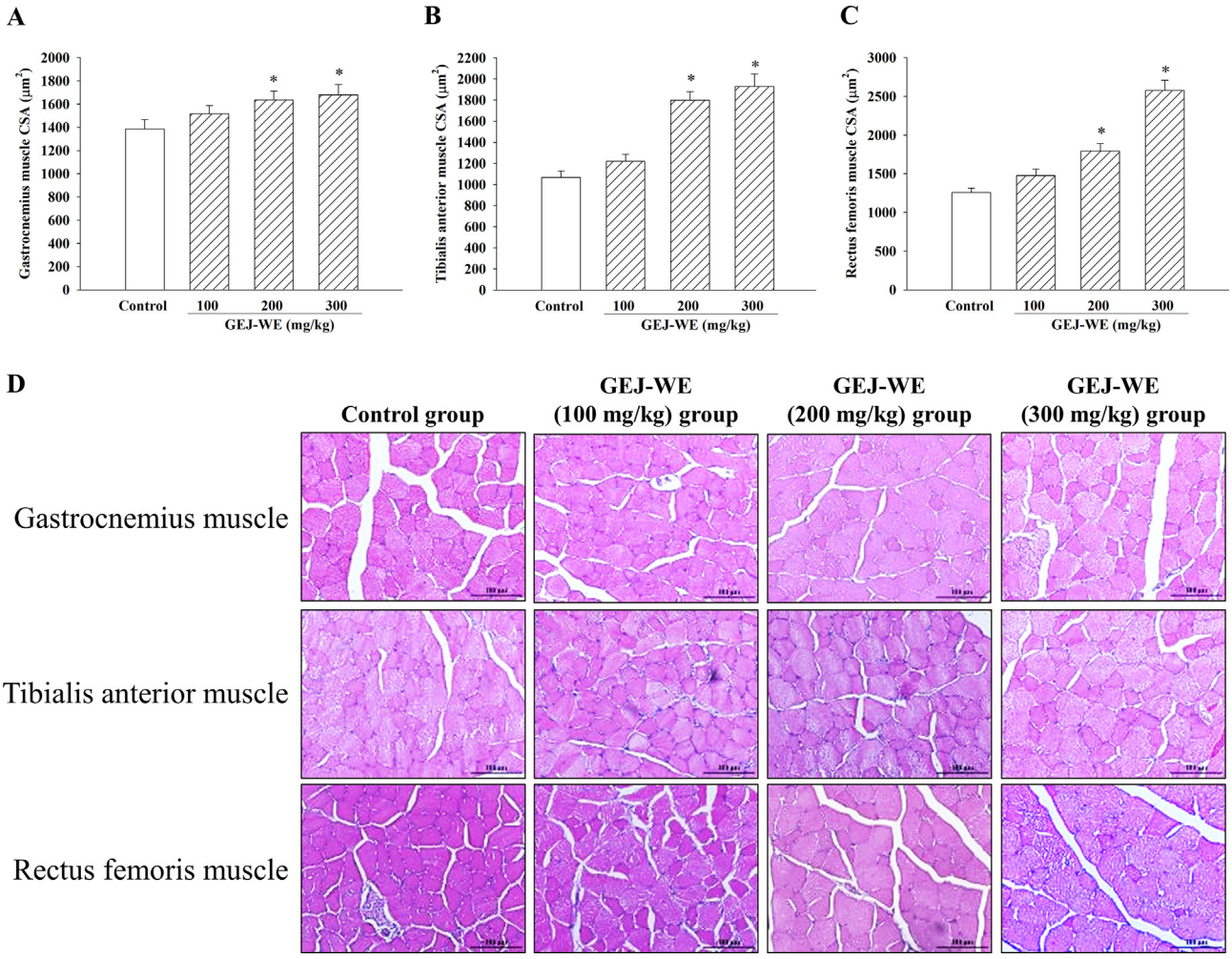

*Fig. 9. **Effects of GEJ-WE on skeletal muscle cross-sectional area (CSA) of gastrocnemius muscle (A), tibialis anterior muscle (B) and rectus femoris muscle (C) of C57BL/6J mice.** Mice were orally treated with vehicle only (saline) or with GEJ-WE (100, 200 and 300 mg/kg/day) for 4 weeks. CSA was measured by hematoxylin and eosin staining in the sections of gastrocnemius muscle (D, top row), tibialis anterior muscle (D, middle row) and rectus femoris muscle (D, bottom row) of C57BL/6J mice at 4-weeks post GEJ-WE treatment. Scale bars = 100 μm. Data represent the mean ± SEM from six independent mice (n = 6 per group). *p < 0.05 vs. control group (vehicle-treated) according to one-way ANOVA followed by a Tukey post hoc test.*

[40]. GEJ-WE (200 and 300 mg/kg/day) significantly increased the proportion of slow-twitch (type I) fibers in the gastrocnemius, tibialis anterior and rectus femoris muscles (Fig. 11) in companied with a reduction of fast-twitch (type II) fibers skeletal muscles compared with control group (Fig. 12). These data indicated that GEJ-WE promoted skeletal muscle fiber type switching from fast-twitch (type II) to slow-twitch (type I), suggesting GEJ-WE increased motor activity and rotarod performance via the increased proportion of slow-twitch (type I) muscle fibers. Moreover, slow-twitch (type I) fibers have higher insulin sensitivity and glucose uptake ability than fast-twitch (type II) fibers and induction of slow-twitch (type I) fibers serve as a therapeutic strategy for treating obesity and type 2 diabetes [41]. Interestingly, we found that GEJ-WE not only increased the proportion of slow-twitch (type I) fibers in skeletal muscles but also decreased both skeletal muscle lipid contents (Fig. S2) and fasting blood glucose levels (Table 2). Moreover, the transition of fiber types is dynamics and affected by many factors. Previous studies have shown that activation of Akt pathway enhances transformation of fast-to-slow-twitch fibers [42,43]. Moreover, PGC-1α is another important regulator that enhanced the formation of slow-twitch (type I) muscle fibers [44,45], leading to enhanced exercise endurance as

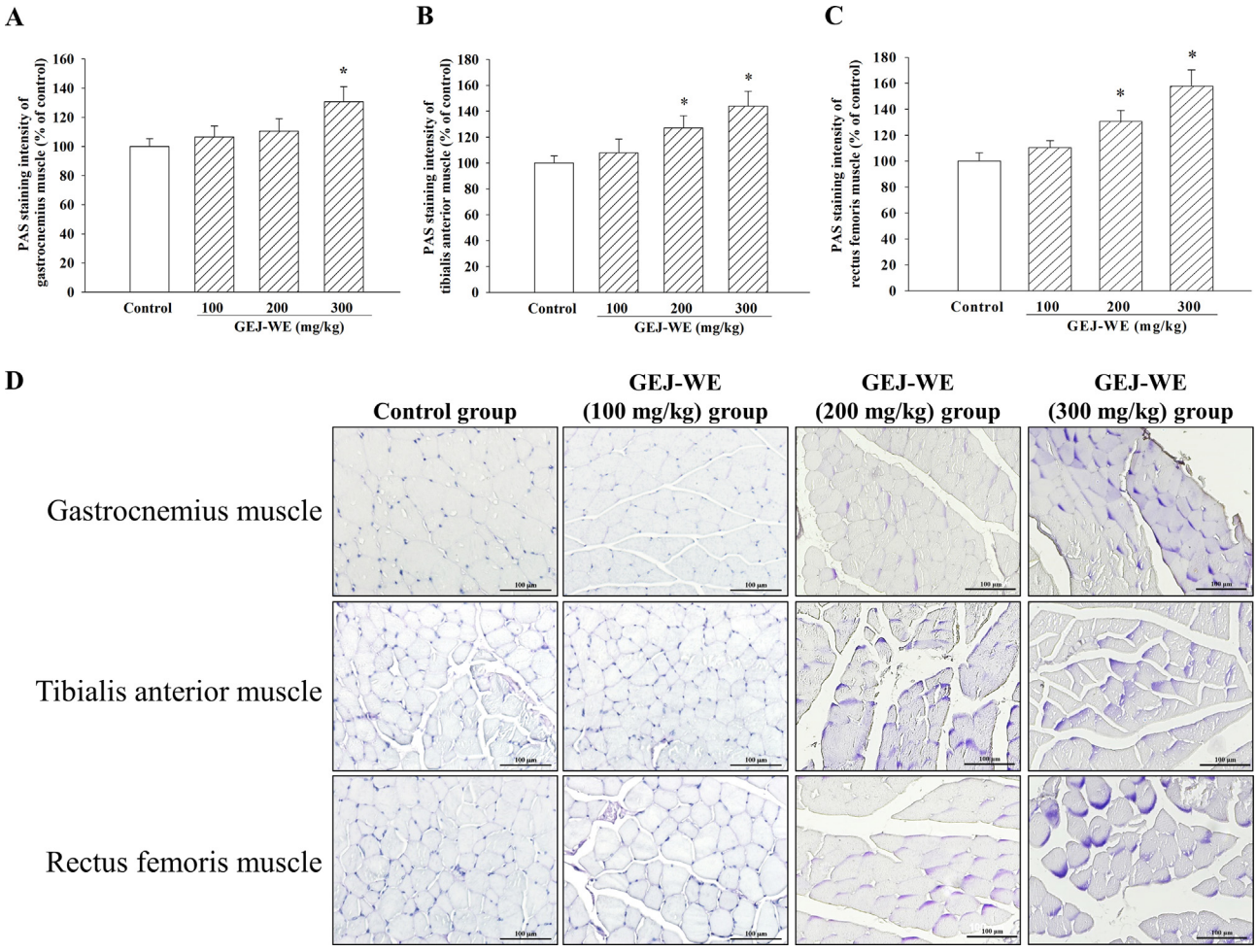

*Fig. 10. **Effects of GEJ-WE on glycogen content of gastrocnemius muscle (A), tibialis anterior muscle (B) and rectus femoris muscle (C) of C57BL/6J mice.** Mice were orally treated with vehicle only (saline) or with GEJ-WE (100, 200 and 300 mg/kg/day) for 4 weeks. Glycogen was measured by PAS staining in the sections of gastrocnemius muscle (D, top row), tibialis anterior muscle (D, middle row) and rectus femoris muscle (D, bottom row) of C57BL/6J mice at 4-weeks post GEJ-WE treatment. Scale bars = 100 μm. Data represent the mean ± SEM from six independent mice (n = 6 per group). *p < 0.05 vs. control group (vehicle-treated) according to one-way ANOVA followed by a Tukey post hoc test.*

measured by rotarod performance [45]. Therefore, GEJ-WE-induced upregulation of p-Akt and PGC-1α might contribute to enhance the transformation of fast-to-slow-twitch fibers leading to greater muscular endurance.

Mitochondria, the "powerhouse of the cell", is involved in the homeostatic regulation of glucose and energy. The dysfunction of mitochondria has been associated with the determining changes in the skeletal muscle mass and function [46]. In skeletal muscle cells, glucose is one of the energy sources for mitochondria-mediated ATP production. Glut4 is the predominantly expressed glucose transporter protein that mediates glucose uptake and it plays a critical role in regulating whole body glucose homeostasis [2]. The translocation of Glut4 to the cell membrane is regulated by IRS-1/Akt signaling which has been shown to play an important role in promoting glycogen synthesis through phosphorylating GSK-3β [47]. The lower muscle glycogen content would decrease muscle functions and further impairs the exercise performance [48]. Our data showed that AG1024 or wortmannin inhibited GEJ-WE-induced upregulation of IRS-1/Akt and p-GSK-3β signaling, Glut4 membrane translocation and glycogen content in myotubes (Fig. 5), suggesting the activation of IGF-1R/Akt signaling contributed to GEJ-WE-induced Glut4 membrane translocation and glycogen synthesis. The activation of IGF-1R/IRS-1/Akt/GSK-3β signaling and the

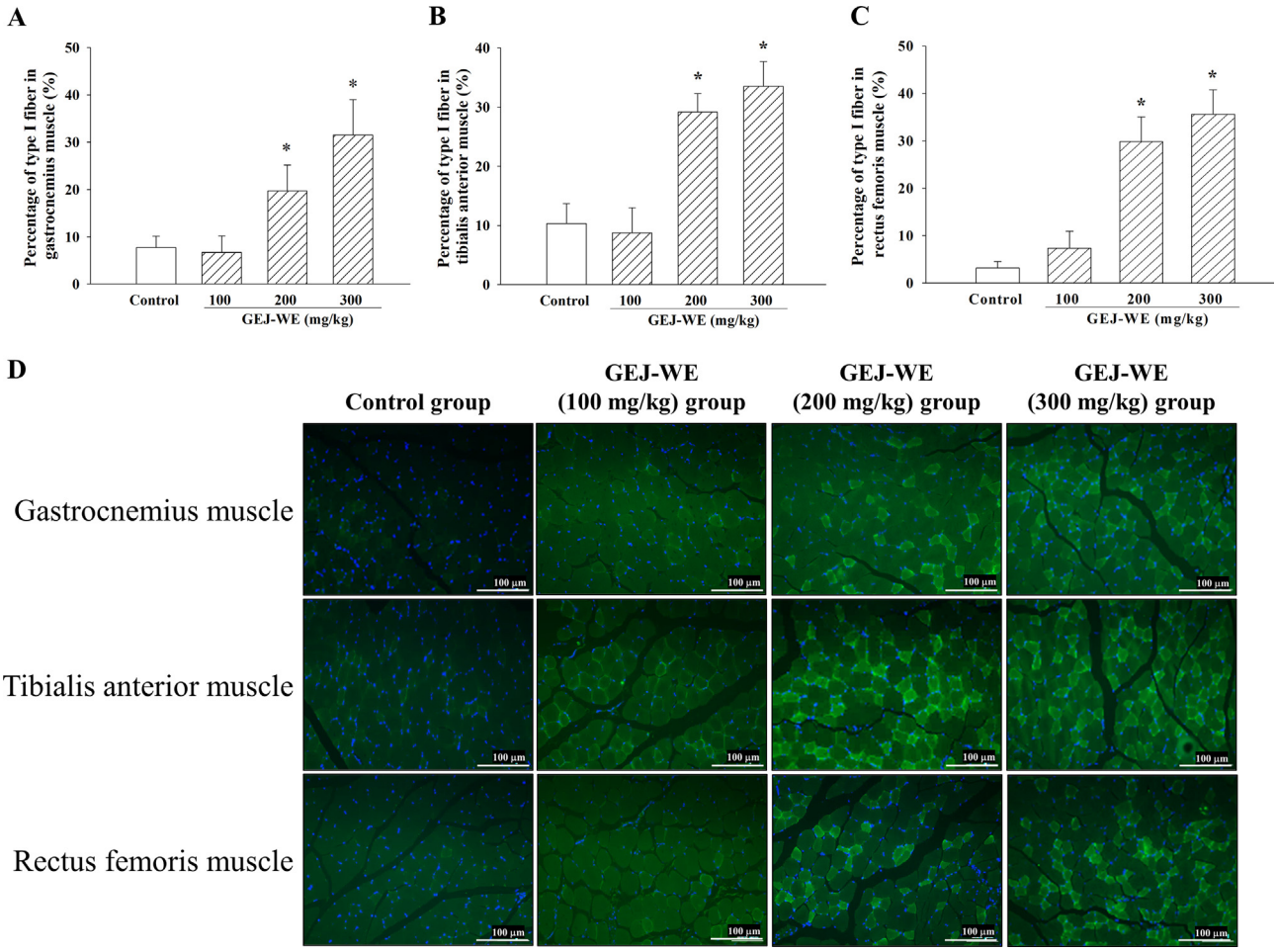

*Fig. 11. **Effects of GEJ-WE on the slow-twitch (type I) fibers of gastrocnemius muscle (A), tibialis anterior muscle (B) and rectus femoris muscle (C) of C57BL/6J mice.** Mice were orally treated with vehicle only (saline) or with GEJ-WE (100, 200 and 300 mg/kg/day) for 4 weeks. Immunofluorescence staining was performed to detect slow-twitch (type I) fibers of gastrocnemius muscle (D, top row), tibialis anterior muscle (D, middle row) and rectus femoris muscle (D, bottom row) of C57BL/6J mice at 4-weeks post GEJ-WE treatment. Scale bars = 100 μm. The proportion of slow-twitch (type I) fiber were manually counted and calculated as total number of slow-twitch (type I) fibers/total number of fibers counted from five randomly selected fields for each sample. Data represent the mean ± SEM from six independent mice (n = 6 per group). *p < 0.05 vs. control group (vehicle-treated) according to one-way ANOVA followed by a Tukey post hoc test.*

increase of glycogen content were also observed in skeletal muscle tissues of GEJ-WE-treated mice, suggesting the potential effects of GEJ-WE on glucose homeostasis in skeletal muscle.

Both *in vitro* and *in vivo* data showed that GEJ-WE significantly upregulated mitochondrial biogenesis signaling related molecules, PGC-1α, NRF1 and TFAM (Figs. 6 and 13), which might contribute to its enhancing effects on mitochondrial activity and ATP production. It is well known that PGC-1α acts as a critical regulator of mitochondrial biogenesis by co-activating with the transcription factor NRF1 to promote TFAM expression [11,46]. In addition, the increase of skeletal muscle glycogen and mitochondrial biogenesis are considered to be the main strategy to reduce muscle fatigue. Our results revealed that mice feed with GEJ-WE increased PGC-1α-mediated mitochondrial biogenesis signaling and Akt/GSK-3β-mediated glycogen content (Fig. 13), which might contribute to its promoting effects on muscle strength and motor performance (Fig. 7). All together, these results suggest that GEJ-WE possesses the beneficial effects on the regulation of mitochondrial biogenesis signaling and glucose homeostasis that contribute to promote skeletal muscle strength and motor performance.

In this work, we identified four amino acids components (L-hydroxyproline, glycine, DL-alanine,

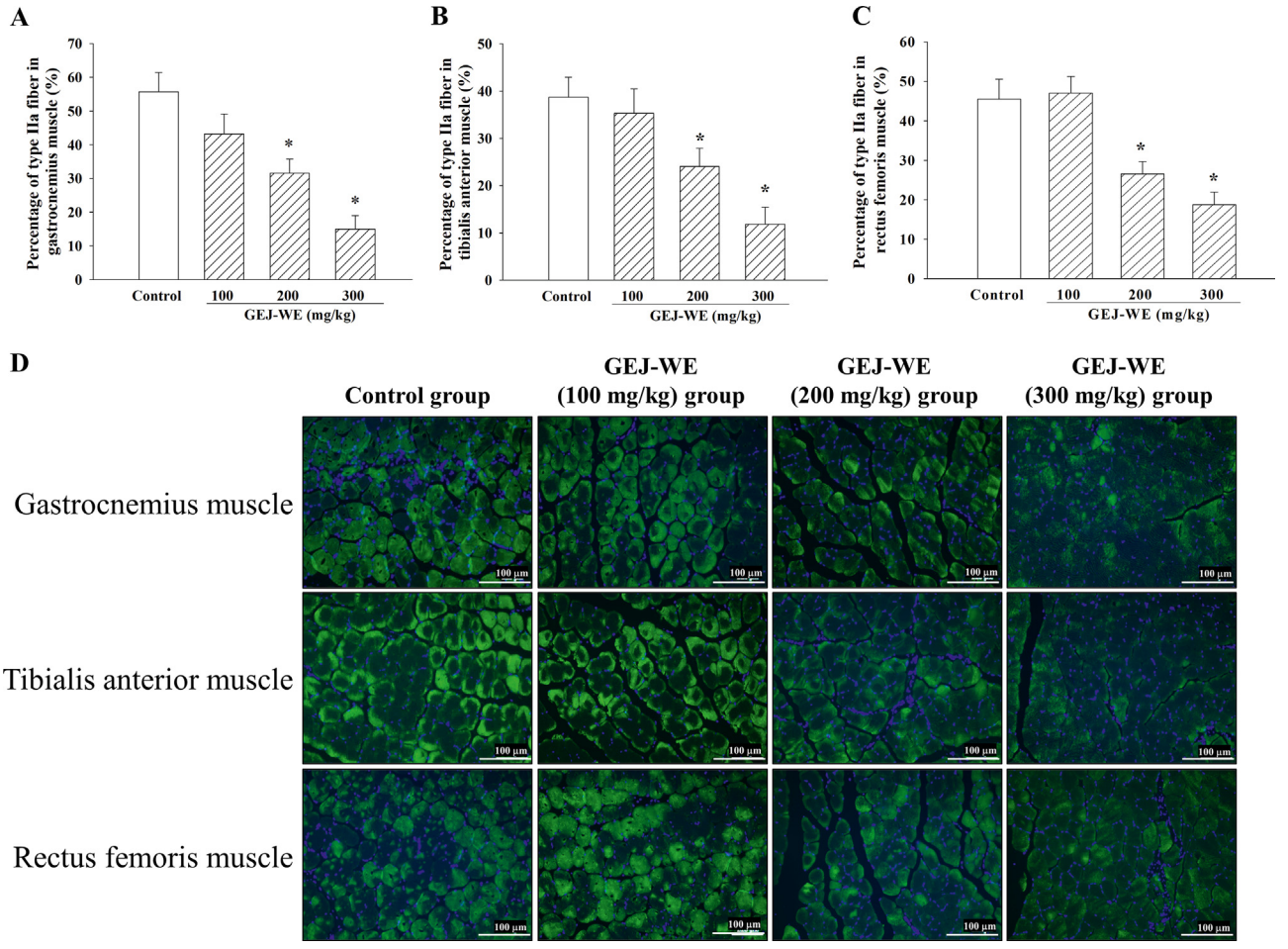

*Fig. 12. **Effects of GEJ-WE on the fast-twitch (type II) fibers of gastrocnemius muscle (A), tibialis anterior muscle (B) and rectus femoris muscle (C) of C57BL/6J mice.** Mice were orally treated with vehicle only (saline) or with GEJ-WE (100, 200 and 300 mg/kg/day) for 4 weeks. Immunofluorescence staining was performed to detect fast-twitch (type II) fibers of gastrocnemius muscle (D, top row), tibialis anterior muscle (D, middle row) and rectus femoris muscle (D, bottom row) of C57BL/6J mice at 4-weeks post GEJ-WE treatment. Scale bars = 100 μm. The proportion of fast-twitch (type II) fiber were manually counted and calculated as total number of fast-twitch (type II) fiber/total number of fibers counted from five randomly selected fields for each sample. Data represent the mean ± SEM from six independent mice ($n = 6$ per group). *$p < 0.05$ vs. control group (vehicle-treated) according to one-way ANOVA followed by a Tukey post hoc test.*

and L-proline) in GEJ-WE (Table 1). Among them, hydroxyproline (a metabolite of proline) and alanine are two important sources for glycine biosynthesis [49]. Glycine has been shown to promote skeletal muscle protein synthesis via activation of Akt/mTOR signaling [50,51]. Furthermore, recent study has shown that hydroxyproline increased the mRNA expression of IGF-1 in skeletal muscle of fish, an important inducer for skeletal muscle protein synthesis [52]. Moreover, they found hydroxyproline increased skeletal muscle fiber density and fiber diameter [52]. In addition, glycine and L-proline have also been reported their enhancing effects on mitochondrial biogenesis via upregulation of PGC-1α/NRF1/TFAM pathway in skeletal muscle [53]. Therefore, amino acids (L-hydroxyproline, glycine, DL-alanine, and L-proline) identified in GEJ-WE play important roles in its promoting effects on skeletal muscle protein synthesis and mitochondrial biogenesis.

In conclusion, GEJ-WE possesses novel enhancing effects on skeletal muscle mass, muscle strength and motor performance via regulation of myogenic differentiation, protein synthesis signaling IGF-1/IGF-1R/IRS-1/Akt, mitochondrial biogenesis signaling PGC-1α/NRF1/TFAM, ATP production, Glut4 translocation, glycogen contents and slow fiber type transition, providing

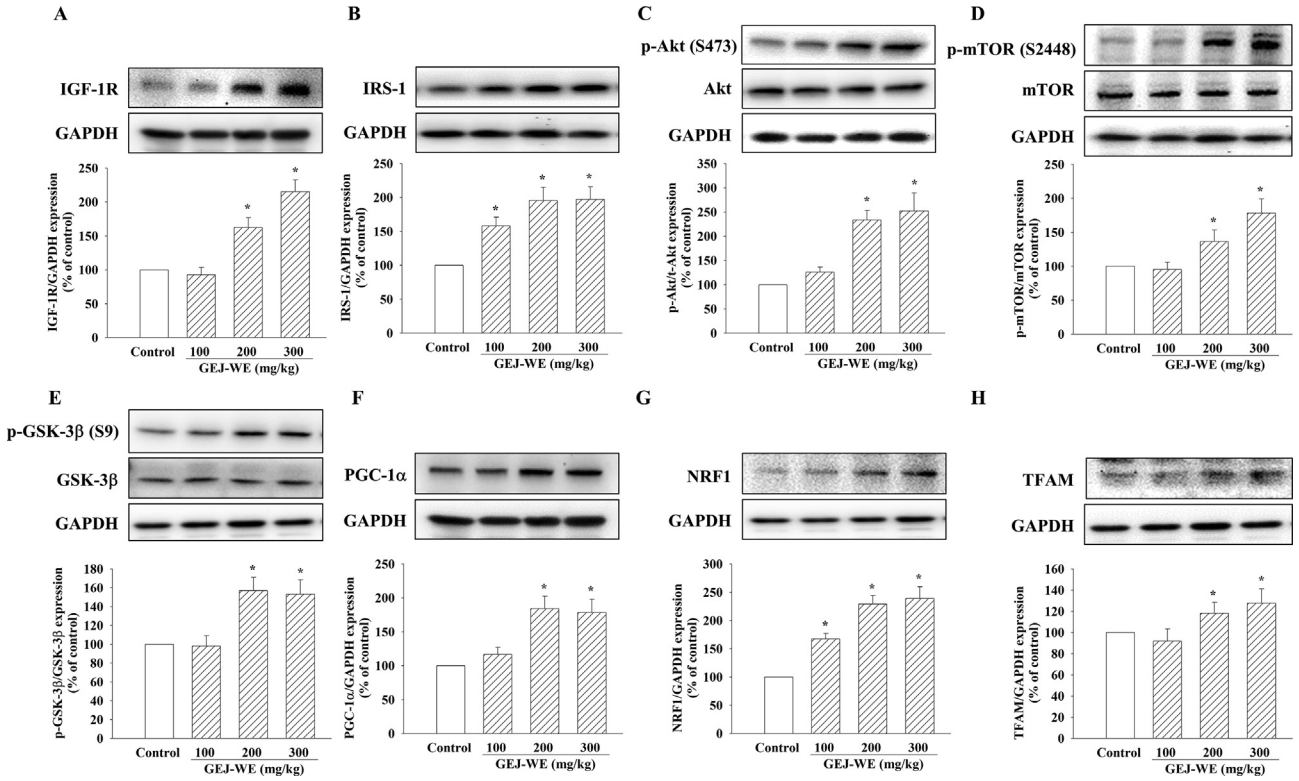

*Fig. 13. **Effects of GEJ-WE on protein expressions of IGF-1R (A), IRS-1 (B), p-Akt (S473)/Akt (C), p-mTOR (S2448)/mTOR (D), p-GSK-3β (S9)/GSK-3β (E), PGC-1α (F), NRF1 (G) and TFAM (H) in tibialis anterior muscle of C57BL/6J mice.** Mice were orally treated with vehicle only (saline) or with GEJ-WE (100, 200 and 300 mg/kg/day) for 4 weeks. Protein expressions were measured by western blotting. Densitometry analyses are presented as the relative ratio of protein/GAPDH or p-protein/protein, and are represented as percentages of matched control group. Data represent the mean ± SEM from six independent mice ($n = 6$). *$p < 0.05$ vs. control group (vehicle-treated) according to Kruskal–Wallis test followed by Dunn's test.*

mechanistic evidence that GEJ-WE enhances skeletal muscle mass and function.

Author contributions

Wei-Yu Fang: Conceptualization, Investigation, Methodology, Formal analysis, Writing-Original Draft. **Wan-Hsuan Chang:** Investigation, Methodology, Formal analysis. **Yi-Hong Tsai:** Investigation, Methodology, Formal analysis, Writing-Original Draft. **Hung-Te Hsu:** Methodology, Writing-Original Draft. **Fang-Rong Chang:** Methodology, Writing-Original Draft. **Chih-Lung Lin:** Resources, Writing-Original Draft. **Yi-Ching Lo:** Conceptualization, Resources, Writing-Review & Editing, Project administration, Funding acquisition. All data were generated in-house, and no paper mill was used. All authors agree to be accountable for all aspects of work ensuring integrity and accuracy.

Conflict of interest

The authors declare that there are no conflicts of interest.

Acknowledgments

This work was supported by Ministry of Science and Technology, Taiwan (grant number MOST 108-2320-B-037-019-MY3). The authors are grateful to Wan-Wen Lo for her excellent assistances.

Appendix. Supplementary methods

Oil Red O Staining

Lipid was visualized on paraffin-embedded tissue sections (5-μm) by Oil Red O staining according to a previous study [54]. Following deparaffinization and rehydration, sections were immersed in Solution 1 (70% ethylene glycol, 5 g linoleic acid and 2 g lecithin) at 56 °C for 3 days. Sections were then rinsed in several changes of 70% ethanol followed by several changes of distilled water for at least 8 h. After that, sections were immersed in Solution 2 (2% chromium trioxide in distilled water) at 4 °C for 24 h followed by rinsed in several changes of distilled water for 24 h. Sections were then immersed in Solution 3 (5% sodium bicarbonate in distilled

water) for 24 h followed by rinsed in water for at least 8 h. After staining with 0.5% Oil Red O in isopropanol for 30 min, sections were rinsed in 60% isopropanol, then rinsed in distilled water, and stained in hematoxylin for 1 min. Images were captured under an optical microscopy (ECLIPSE 80i, Nikon, Japan) and analyzed Oil Red O staining intensity by ImageJ software.

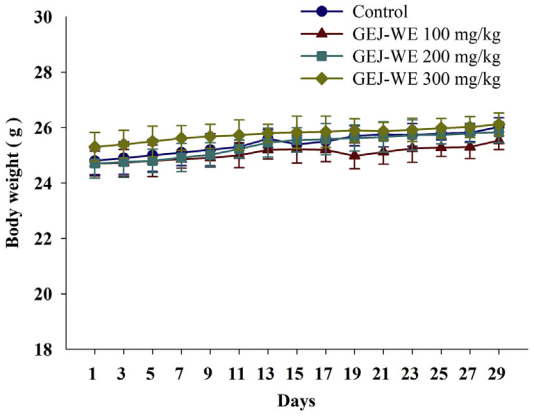

Figure S1. ***Effects of GEJ-WE on growth curve of C57BL/6J mice.*** *Mice were orally treated with vehicle only (saline) or with GEJ-WE (100, 200 and 300 mg/kg/day) for 4 weeks. The body weight of mice were measured every 2 days. Data represent the mean ± SEM from six independent mice (n = 6 per group). *p < 0.05 vs. control group (vehicle-treated) according to one-way ANOVA followed by a Tukey post hoc test.*

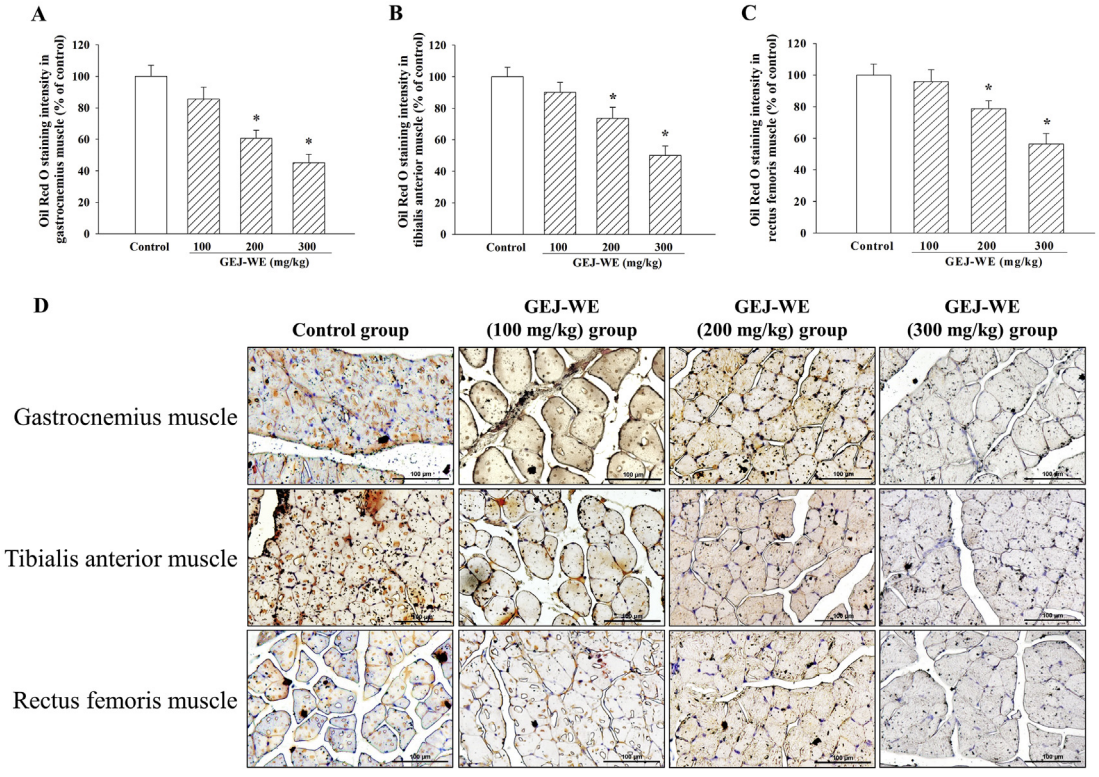

Figure S2. ***Effects of GEJ-WE on lipid content of gastrocnemius muscle (A), tibialis anterior muscle (B) and rectus femoris muscle (C) of C57BL/6J mice.*** *Mice were orally treated with vehicle only (saline) or with GEJ-WE (100, 200 and 300 mg/kg/day) for 4 weeks. Oil Red O staining was used to detect lipid content in the paraffin-embedded tissue sections of gastrocnemius muscle (D, top row), tibialis anterior muscle (D, middle row) and rectus femoris muscle (D, bottom row) of C57BL/6J mice at 4-weeks post GEJ-WE treatment. Scale bars = 100 μm. Data represent the mean ± SEM from six independent mice (n = 6 per group). *p < 0.05 vs. control group (vehicle-treated) according to one-way ANOVA followed by a Tukey post hoc test.*

References

[1] Sartori R, Romanello V, Sandri M. Mechanisms of muscle atrophy and hypertrophy: implications in health and disease. Nat Commun 2021;12:330.

[2] Evans PL, McMillin SL, Weyrauch LA, Witczak CA. Regulation of skeletal muscle glucose transport and glucose metabolism by exercise training. Nutrients 2019;11:2432.

[3] Severinsen MCK, Pedersen BK. Muscle-organ crosstalk: the emerging roles of myokines. Endocr Rev 2020;41:594.

[4] Anker MS, Landmesser U, von Haehling S, Butler J, Coats AJS, Anker SD. Weight loss, malnutrition, and cachexia in COVID-19: facts and numbers. J Cachexia Sarcopenia Muscle 2021;12:9–13.

[5] Sawano S, Mizunoya W. History and development of staining methods for skeletal muscle fiber types. Histol Histopathol 2022:18422.

[6] Mishra P, Varuzhanyan G, Pham AH, Chan DC. Mitochondrial dynamics is a distinguishing feature of skeletal muscle fiber types and regulates organellar compartmentalization. Cell Metabol 2015;22:1033–44.

[7] Wang Y, Pessin JE. Mechanisms for fiber-type specificity of skeletal muscle atrophy. Curr Opin Clin Nutr Metab Care 2013;16:243–50.

[8] Yoshida T, Delafontaine P. Mechanisms of IGF-1-mediated regulation of skeletal muscle hypertrophy and atrophy. Cells 2020;9:1970.

[9] Kido K, Ato S, Yokokawa T, Makanae Y, Sato K, Fujita S. Acute resistance exercise-induced IGF1 expression and subsequent GLUT4 translocation. Physiological Reports 2016;4:e12907.

[10] Hood DA, Memme JM, Oliveira AN, Triolo M. Maintenance of skeletal muscle mitochondria in health, exercise, and aging. Annu Rev Physiol 2019;81:19–41.

[11] Islam H, Edgett BA, Gurd BJ. Coordination of mitochondrial biogenesis by PGC-1alpha in human skeletal muscle: a re-evaluation. Metabolism 2018;79:42–51.

[12] Chou YJ, Chuu JJ, Peng YJ, Cheng YH, Chang CH, Chang CM, et al. The potent anti-inflammatory effect of Guilu Erxian Glue extracts remedy joint pain and ameliorate the progression of osteoarthritis in mice. J Orthop Surg Res 2018;13:259.

[13] Lien CY, Lu CW, Lin YH, Wu WJ, Hsu CH, Chuang TY, et al. Chinese herbal medicine, guilu erxian Glue, as alternative medicine for adverse side effects of chemotherapy in doxorubicin-treated cell and mouse models. Evid Based Complement Alternat Med 2021;2021:5548968.

[14] Kamei Y, Hatazawa Y, Uchitomi R, Yoshimura R, Miura S. Regulation of skeletal muscle function by amino acids. Nutrients 2020;12.

[15] Wang Y, Liu Q, Quan H, Kang SG, Huang K, Tong T. Nutraceuticals in the prevention and treatment of the muscle atrophy. Nutrients 2021;13:1914.

[16] Su W, Fang C, Tseng C, Hung H, Chen Z, Lee H, et al. Therapeutic effect of Guijiajiao (Colla Carapacis et Plastri) on bone regeneration in rats and zebrafish. J Tradit Chin Med 2018;38:197–210.

[17] Lin YH, Chen HY, Li YC, Chiu JC, Yang SH. Adverse events assessment of traditional Chinese herbal product, Guilu Erxian Jiao, in healthy volunteers. J Chin Med 2011;22:65–75.

[18] Tsai CC, Chou YY, Chen YM, Tang YJ, Ho HC, Chen DY. Effect of the herbal drug guilu erxian jiao on muscle strength, articular pain, and disability in elderly men with knee osteoarthritis. Evid Based Complement Alternat Med 2014;2014:297458.

[19] Ma GD, Chiu CH, Hsu YJ, Hou CW, Chen YM, Huang CC. Changbai mountain ginseng (Panax ginseng C.A. Mey) extract supplementation improves exercise performance and energy utilization and decreases fatigue-associated parameters in mice. Molecules 2017;22.

[20] Huang CC, Chen YM, Kan NW, Chao HL, Ho CS, Hsu MC. Cornu cervi pantotrichum supplementation improves exercise performance and protects against physical fatigue in mice. Molecules 2014;19:4669–80.

[21] Kang JY, Kim DY, Lee JS, Hwang SJ, Kim GH, Hyun SH, et al. Korean red ginseng ameliorates fatigue via modulation of 5-HT and corticosterone in a sleep-deprived mouse model. Nutrients 2021;13.

[22] Go GY, Jo A, Seo DW, Kim WY, Kim YK, So EY, et al. Ginsenoside Rb1 and Rb2 upregulate Akt/mTOR signaling-mediated muscular hypertrophy and myoblast differentiation. J Ginseng Res 2020;44:435–41.

[23] Shen L, Haas M, Wang DQ, May A, Lo CC, Obici S, et al. Ginsenoside Rb1 increases insulin sensitivity by activating AMP-activated protein kinase in male rats. Phys Rep 2015;3.

[24] Lee SJ, Bae JH, Lee H, Lee H, Park J, Kang JS, et al. Ginsenoside Rg3 upregulates myotube formation and mitochondrial function, thereby protecting myotube atrophy induced by tumor necrosis factor-alpha. J Ethnopharmacol 2019;242:112054.

[25] Kathirvel E, Morgan K, Nandgiri G, Sandoval BC, Caudill MA, Bottiglieri T, et al. Betaine improves nonalcoholic fatty liver and associated hepatic insulin resistance: a potential mechanism for hepatoprotection by betaine. Am J Physiol Gastrointest Liver Physiol 2010;299:G1068–77.

[26] Ma J, Meng X, Kang SY, Zhang J, Jung HW, Park YK. Regulatory effects of the fruit extract of Lycium chinense and its active compound, betaine, on muscle differentiation and mitochondrial biogenesis in C2C12 cells. Biomed Pharmacother 2019;118:109297.

[27] Szkudelska K, Szkudelski T. The anti-diabetic potential of betaine. Mechanisms of action in rodent models of type 2 diabetes. Biomed Pharmacother 2022;150:112946.

[28] Chen Y, Chen H, Li Y, Chen Z, Wu Y, McGowan E, et al. Chinese herbal medicine Guilu Erxian Jiao attenuates bone marrow suppression following chemotherapy in patients with advanced lung cancer. Translational Metabolic Syndrome Research 2020;3:25–8.

[29] Nair AB, Jacob S. A simple practice guide for dose conversion between animals and human. J Basic Clin Pharm 2016;7:27–31.

[30] Shin EJ, Jo S, Choi S, Cho CW, Lim WC, Hong HD, et al. Red ginseng improves exercise endurance by promoting mitochondrial biogenesis and myoblast differentiation. Molecules 2020;25.

[31] Fang WY, Tseng YT, Lee TY, Fu YC, Chang WH, Lo WW, et al. Triptolide prevents LPS-induced skeletal muscle atrophy via inhibiting NF-kappaB/TNF-alpha and regulating protein synthesis/degradation pathway. Br J Pharmacol 2021;178:2998–3016.

[32] Tseng YT, Chang WH, Lin CC, Chang FR, Wu PC, Lo YC. Protective effects of Liuwei dihuang water extracts on diabetic muscle atrophy. Phytomedicine 2019;53:96–106.

[33] Pedersen BK, Febbraio MA. Muscles, exercise and obesity: skeletal muscle as a secretory organ. Nat Rev Endocrinol 2012;8:457–65.

[34] Hamrick MW, McNeil PL, Patterson SL. Role of muscle-derived growth factors in bone formation. J Musculoskelet Neuronal Interact 2010;10:64–70.

[35] Bikle DD, Tahimic C, Chang W, Wang Y, Philippou A, Barton ER. Role of IGF-I signaling in muscle bone interactions. Bone 2015;80:79–88.

[36] Bower NI, Johnston IA. Transcriptional regulation of the IGF signaling pathway by amino acids and insulin-like growth factors during myogenesis in Atlantic salmon. PLoS One 2010;5:e11100.

[37] Lednev EM, Kravchenko IV, Furalyov VA, Lysenko EA, Lemesheva IS, Grushin AA, et al. Effect of amino acids on IGF1 gene expression in human myotubes and skeletal muscle. Growth Hormone IGF Res 2020;53–54:101323.

[38] Senesi P, Luzi L, Montesano A, Mazzocchi N, Terruzzi I. Betaine supplement enhances skeletal muscle differentiation in murine myoblasts via IGF-1 signaling activation. J Transl Med 2013;11:174.

[39] Go GY, Lee SJ, Jo A, Lee J, Seo DW, Kang JS, et al. Ginsenoside Rg1 from Panax ginseng enhances myoblast differentiation and myotube growth. J Ginseng Res 2017;41:608–14.
[40] Mukund K, Subramaniam S. Skeletal muscle: a review of molecular structure and function, in health and disease, vol. 12. Wiley Interdiscip Rev Syst Biol Med; 2020. p. e1462.
[41] Duan Y, Li F, Tan B, Yao K, Yin Y. Metabolic control of myofibers: promising therapeutic target for obesity and type 2 diabetes. Obes Rev 2017;18:647–59.
[42] Zhang S, Chen X, Huang Z, Chen D, Yu B, Chen H, et al. Leucine promotes porcine myofibre type transformation from fast-twitch to slow-twitch through the protein kinase B (Akt)/forkhead box 1 signalling pathway and microRNA-27a. Br J Nutr 2019;121:1–8.
[43] Wen W, Chen X, Huang Z, Chen D, He J, Zheng P, et al. Lycopene promotes a fast-to-slow fiber type transformation through Akt/FoxO1 signaling pathway and miR-22-3p. J Funct Foods 2021;80:104430.
[44] Lin J, Wu H, Tarr PT, Zhang CY, Wu Z, Boss O, et al. Transcriptional co-activator PGC-1 alpha drives the formation of slow-twitch muscle fibres. Nature 2002;418: 797–801.
[45] Janice Sanchez B, Tremblay AK, Leduc-Gaudet JP, Hall DT, Kovacs E, Ma JF, et al. Depletion of HuR in murine skeletal muscle enhances exercise endurance and prevents cancer-induced muscle atrophy. Nat Commun 2019;10:4171.
[46] Memme JM, Slavin M, Moradi N, Hood DA. Mitochondrial bioenergetics and turnover during chronic muscle disuse. Int J Mol Sci 2021;22:519.
[47] Park JE, Seo Y, Han JS. HM-chromanone, a component of Portulaca oleracea L., stimulates glucose uptake and glycogen synthesis in skeletal muscle cell. Phytomedicine 2021;83:153473.
[48] Vigh-Larsen JF, Ortenblad N, Spriet LL, Overgaard K, Mohr M. Muscle glycogen metabolism and high-intensity exercise performance: a narrative review. Sports Med 2021; 51:1855–74.
[49] Wang W, Wu Z, Dai Z, Yang Y, Wang J, Wu G. Glycine metabolism in animals and humans: implications for nutrition and health. Amino Acids 2013;45:463–77.
[50] Sun K, Wu Z, Ji Y, Wu G. Glycine regulates protein turnover by activating protein kinase B/mammalian target of rapamycin and by inhibiting MuRF1 and atrogin-1 gene expression in C2C12 myoblasts. J Nutr 2016; 146:2461–7.
[51] Liu Y, Wang X, Wu H, Chen S, Zhu H, Zhang J, et al. Glycine enhances muscle protein mass associated with maintaining Akt-mTOR-FOXO1 signaling and suppressing TLR4 and NOD2 signaling in piglets challenged with LPS. Am J Physiol Regul Integr Comp Physiol 2016;311:R365–73.
[52] Cao S, Xiao Y, Huang R, Zhao D, Xu W, Li S, et al. Dietary supplementation with hydroxyproline enhances growth performance, collagen synthesis and muscle quality of Carassius auratus triploid. Front Physiol 2022;13:913800.
[53] D'Antona G, Ragni M, Cardile A, Tedesco L, Dossena M, Bruttini F, et al. Branched-chain amino acid supplementation promotes survival and supports cardiac and skeletal muscle mitochondrial biogenesis in middle-aged mice. Cell Metabol 2010;12:362–72.
[54] Tracy RE, Walia P. Lipid fixation for fat staining in paraffin sections applied to lesions of atherosclerosis. Virchows Arch 2004;445:22–6.